Chair of Communication Networks
Aachen University of Technology
Prof. Dr.-Ing. B. Walke

Diploma Thesis

Performance Evaluation of SDMA Coordination Schemes for WiMAX Systems

by

Francisco Niño Álvarez

Matriculation Number: 285010

Aachen, April 28, 2009

Supervised by:
o. Prof. Dr.-Ing. B. Walke
Dipl.-Ing. Benedikt Wolz
Dipl.-Ing. Karsten Klagges

I assure that I have done this work entirely on my own without any further assistance but the official support of the Chair of Communication Networks. All the literature used is listed in the bibliography.

Aachen, April 28, 2009

(Francisco Niño Álvarez)

ABSTRACT

Advanced antenna technologies that are technically mature are currently being integrated into modern wireless systems such as WiMAX or LTE. Capacity and service quality provided by wireless links, as well as the spectral efficiency, are expected to be significantly boosted by advanced antenna techniques that are using multiple antennas either at the transmitter, at the receiver or at both sides.
Beamforming or Space Division Multiple Access (SDMA) techniques are able to simultaneously transmit different signals to different receivers. Furthermore, concurrent reception of different signals is provided by joint detection techniques. In this manner the Medium Access Control (MAC) layer can also schedule stations separated in space. Thus, the capacity of the system can be increased with the number of concurrent data streams. But an SDMA enabled cell generates more varying interference than a conventional cell, because a changing number of subscriber stations are sending uplink data in parallel or DL streams with changing direction are transmitted by the base station. Thereby the SINR estimation becomes less precise and the link adaptation less effective.
This thesis investigates schemes for mitigating inter-cell interference and increasing the precision of SINR estimations in SDMA enhanced system. Three concepts of coordination of BS are developed, implemented and evaluated in this work. System level simulations are conducted in a cellular deployment by means of the open Wireless Network Simulator (openWNS). They show the considerable gain of the developed enhancements compared to an uncoordinated system.

KURZFASSUNG

Diese Arbeit untersucht Methoden zur Reduzierung der Interferenz zwischen Gleichkanalzellen und zur Erhöhung der Schätzgenauigkeit des Störabstandes in um räumlichen Vielfachzugriff erweiterten (SDMA) Systemen. Drei Konzepte für die Koordinierung von Basisstationen sind entwickelt, implementiert und bewertet in dieser Arbeit. Systemlevel-Simulation werden in einem zellularen Umgebung durchgeführt mit Hilfe des open Wireless Network Simulators (openWNS). Diese zeigen den teilweise beträchtlichen Gewinn der entwickelten Erweiterungen im Vergleich zu unkoordinierten Systemen.

CONTENTS

CHAPTER 1

Introduction

1.1 Broadband Wireless Access

Nowadays, services such as video applications, social networks, file sharing, games and voice over IP have become a costumers' necessity. These services require a broadband capacity. Digital Subscriber Line (DSL) family, Fiber to the Home (FTTH), Broadband over Power Lines (BPL) or Broadband Wireless Access (BWA) are the chosen technologies in order to satisfy the costumer's demand services.
Currently, wired technologies are widely accessible in the developed and much of the developing world. Where the traditional wired infrastructures have physical limitations or where the deployment is difficult for wired infrastructure to reach, fixed BWA becomes an ideal technology to set up. Furthermore, due to the quick deployment and the reasonable installation costs to support high rate access of fixed BWA technology, it represents an useful technology for the operators to penetrate new markets.
Besides the required broadband capacity, in the next years, the costumers will demand portable and mobile broadband, it means broadband access everywhere. The wireless technology as well as fixed access, offers the potential to provide portable and mobile access. Up to now, they cover large areas with narrow band access (2nd Generation (2G) and 3rd Generation (3G)) or local areas with broadband access (Wireless Local Area Network (WLAN)s). Worldwide Interoperability for Microwave Access (WiMAX) is promising to cover large regions with a broadband access.

1.2 Motivation - Predictability and mitigation of Inter-cell interference

Multi-antenna techniques and espeacially beamforming and SDMA are an important part of new wireless systems. Computer simulations show potencial gains of SDMA technology in terms of throughput, packet delay and coverage range [18].
In such sytems, due to simultaneous transmissions in co-channel cells, the inter-cell interference becomes the limiting factor[18]. Interference scales with the number of concurrent active SDMA Subscriber Station (SS)s and becomes highly variable. In Downlink (DL), the perceived interference at a SS varies depending if the interfering Base Station (BS)s direct mainlobes or zeros towards this SS. The link adaptation is based on the estimated Signal-to-Interference-and-Noise Ratio (SINR), therefore an accurate inter-cell interference estimation is necesarry to obtain a reliable link adapatation.
The main goal of this thesis is the design and performance evaluation of a concept to allow to increase the predictability of the inter-cell interference and to mitigate its strength.

1.3 Outline of the thesis

Chapter 2 gives an overview of the IEEE 802.16 standards and their history, focused on IEEE 802.16e, 802.16j and 802.16m. Chapter 3 introduces beamforming and related techniques to enable SDMA and presents the SDMA scheduling concept. Chapter 4 introduces the coordination schemes designed. Chapter 5 presents the new methods and

classes implemented within openWNS. In chapter 6 the multi-cell scenario, the different performance metrics and the WiMAC simulation setup are presented. The simulation results obtained by using the coordination schemes are detailed presented and compared with an uncoordinated system. Finally, chapter 7 presents the conclusions and gives some ideas to improve the coordination schemes applied.

CHAPTER 2

IEEE 802.16

In this chapter the IEEE 802.16 is introduced, focused on the standards IEEE 802.16e, 802.16j and 802.16m which are the bases of this thesis.

2.1 Overview [8]

IEEE 802 defines international standards, to be recognized by the International Organization for Standardization (ISO) later, e.q., Metropolitan Area Network (MAN). IEEE 802 projects generally deal with the Physical Layer (PHY) transmission and Medium Access Control (MAC). One of the wireless standards in the 802 Project is the IEEE 802.16 Wireless Metropolitan Area Network (WMAN);
The concept for WMAN has been introduced in recent years. Of the many efforts, the IEEE 802.16 standard originally defining Fixed Broadband Wireless (FBW) is widely considered a new generation technology to replace the past Wireless Local Loop (WLL) in telecomunications, and to deliver performance comparable to traditional cable, T1, DSL, etc. The advantages of IEEE 802.16 include:

- quick deployment, even in those areas where it is difficult for wired infrastructure to reach;
- the ability to overcome physical limitation of traditional wired infrastructure;
- reasonable installation costs to support high rate acces.

WiMAX Forum is a non-profit corporation formed by equipment and component suppliers to promote the adoption of IEEE 802.16-compliant equipment by operators of broadband wireless access systems, which is comparable to the *WiFi Alliance* in promoting IEEE WLANs. WiMAX is establishing '*System Profiles*' for all compliant equipment, which can also address regulatory spectrum constraints faced by operators in different geographical regions. The *WiMAX Forum* is also developing higher-layer specifications to match IEEE 802.16. In the meantime, WiMAX-defining conformance tests in conjunction with interoperability enable service providers to choose multiple vendors.
In April 2002, IEEE 802.16 was published for 10-66 GHz operations, while Line-of-Sight (LOS) transmission is considered a primary application. To promote immediate wider applications, IEEE 802.16a was published in January 2003, which aims at 2-11 GHz operations for Non-Line-of-Sight (NLOS) performance.
FBW access applications based on point-to-multipoint network topology primarily include:

- cellular (or Fixed-Network) backhaul;
- broadband on demand;
- residential broadband;
- underserved areas services;
- normadic wireless services.

As a consequence, FBW (later refined as BWA, for the IEEE 802.16) systems and networks supports:

- high throughput;
- high degree of scalability;
- Quality of Service (QoS) capability;
- high degree of security;
- excellent radio coverage.

IEEE 802.16 WMAN has a connection-oriented MAC and PHY is based on NLOS radio operation in 2-11 GHz. For licensed bands, channel bandwidth will be limited to the regulatory provisioned bandwidth divided by any power of 2, no less than 1.25MHz. Three technologies have been defined:

- Single Carrier (SC);
- Orthogonal Frequency Division Multiplexing (OFDM);
- Orthogonal Frequency Division Multiple Access (OFDMA).

The communication of frame-based IEEE 802.16 is based on the fundamental concept by defining burst profiles in each BS-SS communication link.
IEEE 802.16 had a revision published in October 2004, which is known as IEEE 802.16-2004. The mobile version of IEEE 802.16 has been developed in the IEEE 802.16e, which is commonly known as *Mobile WiMAX*, especially considering its OFDMA PHY. At the ITU. Radiocommunication Sector (ITU-R) May 2007 meeting in Japan, *Mobile WiMAX* was recommended as OFDMA Time Division Duplex (TDD) WMAN, thus leaving 50MHz bandwidth internationally available at 2.57-2.62 GHz from 3G TDD spectrum, on a per nation basis.
Since March 2006, the IEEE 802.16 working group has devoted a task group to incorporating relay capabilities in the foundation of *Mobile WiMAX*. This task group is currently in the process of finishing IEEE 802.16j, the Multihop Relay Specification for 802.16. This addendum will be fully compatible with 802.16e mobile and subscriber stations, but a base station specific to 802.16j will be required for relays to operate.
Since December 2006, IEEE 802.16m has started as new amendment project to study the IEEE 802.16 WMAN-OFDMA specification to provide an advaced air interface for operation in licented bands, and to meet the cellular layer requirements for IMT-Advanced for the next generation of mobile networks with continuing support for legacy WMAN-OFDMA equipment and devices.

2.2 IEEE 802.16e Mobility[2]

This amendment enhances IEEE Standard 802.16-2004 by providing additional specifications required to support mobile as well as fixed terminals.
This standard will increase the market for BWA solutions by taking advantage of the inherent mobility of wireless media. It will fill the gap between very high data rate wireless local area networks and very high mobility cellular systems. It will support fixed and mobile services for both enterprise and consumer markets.

2.3 IEEE 802.16j Mobile Multi-hop Relay Task Group[6]

The purpose of this amendment is to enhance coverage, throughput and system capacity of 802.16 networks by specifying 802.16 multihop relay capabilities and functionalities of interoperable relay stations and base stations.
The multihop relay is a promising solution to expand coverage and to enhance throughput and system capacity for IEEE 802.16 systems. It is expected that the complexity of

relay stations will be considerably less than the complexity of legacy IEEE 802.16 base stations. The gains in coverage and throughput can be leveraged to reduce total deployment cost for a given system performance requirement and thereby improve the economic viability of IEEE 802.16 systems. Relay functionality enables rapid deployment and reduces the cost of system operation. These advantages will expand the market opportunity for broadband wireless access. This project aims to enable exploitation of such advantages by adding appropriate relay functionality to IEEE Std 802.16 through the proposed amendment. Stakeholders include manufacturers and operators of IEEE 802.16 networks.

2.4 IEEE 802.16m Advanced Air Interface[4]

This standard amends the IEEE 802.16 WirelessMAN-OFDMA specification to provide an advanced air interface for operation in licensed bands. It meets the cellular layer requirements of IMT-Advanced next generation mobile networks. This amendment provides continuing support for legacy WirelessMAN-OFDMA equipment.
The ITU-R, is developing the IMT-Advanced radio interface standards to provide advanced air interface specifications for mobile telecommunications. The proposal for IMT-Advanced were solicited in January 2009, and under the current schedule standardization is expected to continue through 2009. This project will seek to develop an advanced IEEE 802.16 air interface by working cooperatively with ITU-R and its members.

CHAPTER 3

Introduction to SDMA

In the first part of the chapter beamforming and related techniques to enable SDMA are introduced. In the second part, the SDMA scheduling is introduced.

3.1 Smart antennas and beamforming

Smart or adaptive antennas control their pattern, by means of feedback control, while the antenna is operating [9]. Smart antennas are constructed as arrays or as continuous aperture antennas. But because the pattern of an array is easily controlled by adjusting the amplitude and phase of the signal of each element before the transmissions, smart antennas are built as arrays rather than continuous aperture antennas. The position of the individual antenna elements has a specific geometric layout (e.g. on a line or circle), and the distances between the elements are typically on a scale of $\lambda/2$, where λ is the wavelength of the carrier signal. Generally, only the fixed stations have antenna arrays because antenna arrays are too big and too costly for mobile terminals. [18]

Smart Antennas at the Base Station

A smart antenna at the BS can be used to improve the link quality for a single data stream in Uplink (UL) (Single Input Multiple Output (SIMO)) and DL (Multiple Input Single Output (MISO)). It may also be used to form multiple adaptive beams to provide SDMA for different SS at the same time [18].

Smart Antennas at the Base Station and Subscriber Station

In the scenario with smart antennas at BS and SS, one link is then a point-to-point Multiple Input Multiple Output (MIMO) system. If several links are concurrently active, it is a Multi-User Multiple Input Multiple Output (MU MIMO) system [18].

3.1.1 Benefits of Smart Antennas

Smart antennas are usually used at the BS for UL reception and DL transmission with multiple antennas. Smart/adaptive antennas allow spatial access to the radio channel by means of different approaches, for example, based on directional parameters or by exploiting the second-order spatial statistics of the radio channel. Thus, space-time processing reduces interference and enhances the desired signal. Moreover, adaptive antennas can exploit long-term and/or short-term properties of the mobile radio channel to achieve improved channel estimation accuracy and reduced computational complexity [16]. The gains achievable with multiple antenna systems on the transmit side as well as the receive side can be classified as follows [21]:

- The array (or Beamforming) gain is the average increase in signal power at the receiver due to a coherent combination of the signal received at all antenna elements. It is proportional to the number of Receiver (Rx) antennas. If channel knowledge

is available at the transmitter, the array gain can also be exploited in systems with multiple antennas at the transmitter.
- The achievable diversity gain depends on the number of Transmitter (Tx) and Rx antennas as well as the propagation channel characteristics, that is, the number of independently fading branches (diversity order). The maximum diversity order of a flat-fading MIMO channel is equal to the product of the number of Rx and Tx antennas. Tx diversity with multiple transmit antennas can, for instance, be exploited via space-time coding and does not require any channel knowledge at the transmitter.
- The interference reduction (or avoidance) gain can be achieved at the receiver and the transmitter by (spatially) suppressing other co-channel interferers. It requires an estimate of the channel of the desired user.
- The spatial multiplexing gain can be obtained by sending multiple data streams to a single user in a MIMO system or to multiple co-channel users in an SDMA system. These techniques take advantage of several independent spatial channels through which different data streams can be transmitted.

Multiple antennas at the BS and also at high performance terminals achieve significantly higher data rates, better link quality, and increased spectral efficiency [17]. Hence, more users can be accommodated by the system and a corresponding capacity increase achieved. To obtain very high data rates, MIMO processing techniques such as spatial multiplexing and space-time coding can be used[13]. MIMO techniques can also be used in order to reduce the total transmitted power, preserving the data rate and, then, reducing the overall system interference. Overall, the adoption of MIMO processing techniques in future wireless systems is expected to have a significant impact on the efficient use of spectrum, the minimization of the cost of establishing new wireless networks, on the optimization of the service quality provided by those networks, and to facilitate the realization of transparent operation across multitechnology wireless networks. Performance enhancements achieved by the se of multiple Tx and/or Rx antennas in wireless telecommunications can be summarized as follows [22]:

- Increase of channel (and hence system) capacity.
- Decrease of the Bit Error Ratio (BER) without any bandwidth expansion or Tx power increases when Rx diversity and space-time linear processing or coding, that is, Tx diversity, are used jointly, or alternatively with cell range expansion if performance is traded-off for coverage.
- Decrease of the impact of fading effects.
- Decrease of total transmitted power/system interference for the same data rates.
- Increase of the packet call and cell throughput at the system level.
- Improvement of coverage for high data rates.

3.1.2 Smart Antenna Algorithms[18]

This section introduces algorithms that are used by antenna arrays, focused on beamforming algorithms.

3.1.2.1 Diversity Coding

Diversity exploits the random nature of radio propagation by finding independent or at least highly uncorrelated signal paths for communication. If one radio path undergoes

a fade, another independent path may have a strong signal. By decreasing the sensitivity to fading, diversity coding allows the use of higher-level modulation to increase the effective data rate. It is effective when the system capacity is limited by multipath fading. Common forms of diversity are:

- **Temporal diversity:** Replicas of the signal are transmitted in different time slots, where the separation between the time slots is greater than the coherence time of the channel.
- **Frequency diversity:** Replicas of the signal are transmitted in different frequency bands, where the separation between the frequency bands is greater than the coherence bandwidth of the channel.
- **Antenna diversity:** Antennas with large enough spacing lead to uncorrelated channels. The transmission of replicas of the signal over these spatial channels leads to spatial diversity.

3.1.2.2 Spatial Multiplexing

By means of spatial multiplexing two SSs with n antennas each, are able to establish up to n orthogonal channels between each other. Each channel has about the same data rate as that of a single Single Input Single Output (SISO) channel.

3.1.2.3 Spatial Filtering and Interference Cancelation

The algorithms described in the following refer to a common signal model, which is described below. The beamforming algorithms introduced thereafter are narrow-band beamformers.

Signal Model and Array Covariance Matrix

Consider an array of M omnidirectional elements immersed in a homogeneous media in the far field of M uncorrelated sinusoidal point sources of frequency f_0. Let the origin of the coordinate system be taken as the time reference (refer to Figure 3.1). Thus, the time taken by a plane wave arriving from i^{th} source in direction (ϕ_i, θ_i) and measured from the l^{th} element to the origin is given by

$$\tau_l(\phi_i, \theta_i) = \frac{\vec{r}_l \cdot \hat{\vec{v}}(\phi_i, \theta_i)}{c} \tag{3.1}$$

where $\vec{r}_l$ is the position of the l^{lth}, $\vec{r}_l \cdot \hat{\vec{v}}(\phi_i, \theta_i)$ is the unit vector in direction (ϕ_i, θ_i), and c is the speed of propagation of the plane wave front. For a linear array of equispaced elements with elements spacing Δx aligned with the x-axis such that the first element is situated at the origin, it becomes

$$\tau_l(\phi_i, \theta_i) = \frac{\Delta x}{c} l \cos(\phi_i) \sin(\theta_i) \tag{3.2}$$

The signal induced on the reference element due to the i^{th} source is normally expressed in complex notation as

$$m_i(t) e^{j2\pi f_0 t} \tag{3.3}$$

with $m_i(t)$ denoting the complex modulation function. Assuming that the wavefront on the l^{th} element arrives $\tau_l(\phi_i, \theta_i)$ seconds before it arrives at the reference element, the signal induced on the l^{th} element due to the i^{th} source can be expressed as

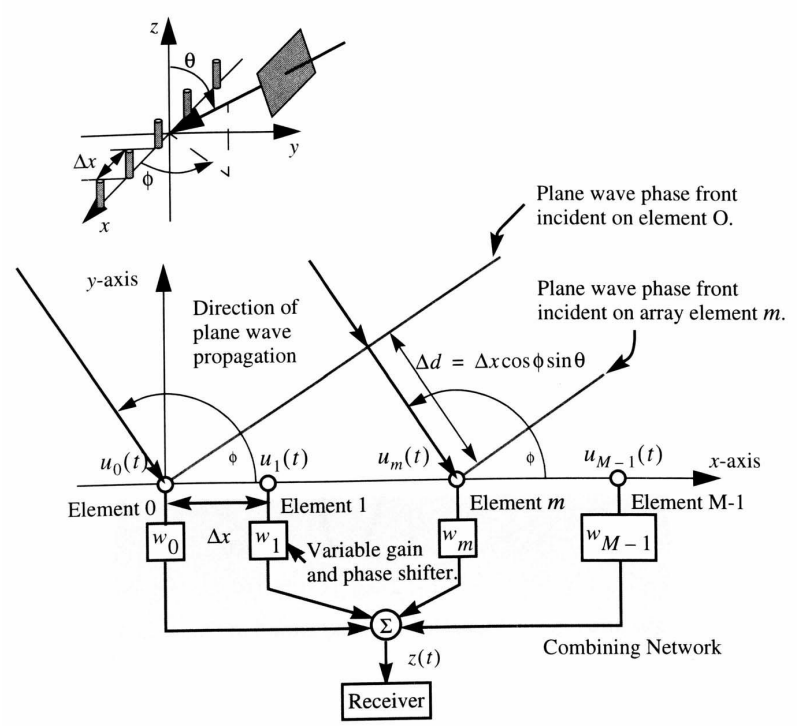

Figure 3.1: Plane Wave incident on Uniform Linear Array [20]

$$m_i(t)e^{j2\pi f_0(t+\tau_l(\phi_i,\theta_i))} \tag{3.4}$$

The expression is based upon the narrow-band assumption for array signal processing, which assumes that the array dimensions are small enough for the modulating function to stay almost constant during $\tau_l(\phi_i, \theta_i)$ seconds, that is, the approximation $m_i(t) \approx m_i(t + \tau_l(\phi_i, \theta_i))$ holds. Figure 3.1 illustrates the scenario. Let x_1 denote the total signal induced due to all N directional sources and background noise on the l^{th} element. Then it is given by

$$x_1 = \sum_{i=1}^{N} m_i(t)e^{j2\pi f_0(t+\tau_l(\phi_i,\theta_i))} + n_l(t) \tag{3.5}$$

where $n_l(t)$ is a random noise component on the l^{th} element, which includes background noise and electronic noise generated in the l^{th} channel. It is assumed to be temporally white with zero mean and variance σ_n. Consider the narrow-band beamformer of Figure 3.1, where signals from each element are multiplied by a complex weight w_l and summed to form the array output. The array output is given by

$$z(t) = \sum_{l=0}^{M-1} w_l^* x_l(t) \tag{3.6}$$

where * denotes the complex conjugate. Denoting the weights of the beamformer as

$$\vec{w} = (w_0, w_1, \ldots, w_{M-1})^T \tag{3.7}$$

and signals induced on all elements as

$$\vec{x} = (x_0, x_1, \ldots, x_{M-1})^T \tag{3.8}$$

the output of the beamformer becomes

$$z(t) = \vec{w}^H \vec{x}(t). \tag{3.9}$$

The notation w^H denotes the Hermitian adjoint (complex conjugate transpose) of w. If the components of $\vec{x}(t)$ can be modeled as zero mean stationary processes, then for a given $\vec{w}$ the mean output power of the processor is given by

$$P(\vec{w}) = E[z(t)z^*(t)] = \vec{w}^H R \vec{w} \tag{3.10}$$

where $E[\cdot]$ denotes the expectation operator and R is the array correlation matrix defined by

$$R = E[\vec{x}(t)\vec{x}^H]. \tag{3.11}$$

Elements of this matrix denote the correlation between various elements. Denote the steering vector associated with the direction (ϕ_i, θ_i) of the i^{th} source by an M-dimensional complex vector $\vec{s}_i$ as

$$\vec{s}_i = (e^{j2\pi f_0 \tau_0(\phi_i,\theta_i)}, \ldots, e^{j2\pi f_0 \tau_{M-1}(\phi_i,\theta_i)})^T. \tag{3.12}$$

Then R can be expressed as

$$R = \sum_{i=1}^{N} p_i \vec{s}_i \vec{s}_i^H + \sigma_n^2 I \tag{3.13}$$

where I is the identity matrix and p_i denotes the power of the i^{th} source measured at one of the elements of the array. p_i is the variance of the complex modulating function $m_i(t)$ when it is modeled as a zero mean low-pass random process. Using matrix notation, the correlation matrix R may be expressed in the following compact form:

$$R = ASA^H + \sigma_n^2 I \tag{3.14}$$

where columns of the $M \times N$ matrix S denotes the source correlation. For uncorrelated sources, it is a diagonal matrix with

$$S_{ij} = \begin{cases} p_i, i = j \\ 0, i \neq j \end{cases} \tag{3.15}$$

Sometimes, it is useful to express R in terms of its eigenvalues and their associated eigenvectors. The eigenvalues of R can be divided into two sets when the environment consists of uncorrelated directional sources and uncorrelated white noise. The eigenvalues contained in one set are of equal values. Their value does not depend upon the directional sources and is equal to the variance of the white noise. The eigenvalues contained in the second set are a function of the parameters of the directional sources, and their number is equal to the number of these sources. Each eigenvalue of this set is associated with a directional source, and its value changes with the change in the source power of this source. The eigenvalues of this set are bigger than those associated with white noise. Sometimes, these eigenvalues are referred to as the signal eigenvalues, and the others belonging to the first set are referred to as the noise eigenvalues. Thus, the R of an array of M elements immersed in N directional sources and the white noise has N signal eigenvalues and $M - N$ noise eigenvalues. R can be spectrally decomposed into

$$R = \sum_{l=1}^{M} \lambda_l \vec{U}_l \vec{U}_l^H + \sigma_n^2 I, \tag{3.16}$$

where the λ_l are the eigenvalues and $\vec{U}_l$ the corresponding unit-norm eigenvectors.

Conventional Beamforming

A conventional beamformer applies weights of equal magnitude. The phases are selected to steer the array in a particular direction (ϕ_0, θ_0), known as the look direction. With $\vec{(}s_0)$ denoting the steering vector in the look direction, the array weights are given by

$$\vec{w}_0 = \frac{1}{M}\vec{s}_0. \tag{3.17}$$

The array with these weights has unity response in the look direction, that is, the mean output power of the processor due to a source in the look direction is the same as the source power arriving at the array (input power). The signals received at the antenna elements are added up in phase. In an environment consisting of only uncorrelated noise and no directional interferences, this beamformer provides maximum Signal-to-Noise Ratio (SNR). For uncorrelated noise, the noise covariance matrix is given by $R_N = \sigma_n^2 I$ and the output noise power of the beamformer

$$P_N = \vec{w}_c^H R_N \vec{w}_c = \frac{\sigma_n^2}{M}. \tag{3.18}$$

This shows that the noise power at the array output is M times less than that present on each element. Thus, the processor with unity gain in the signal direction has reduced the uncorrelated noise by M, yielding the output $SNR = p_s M/\sigma_n^2$. As the input SNR is p_s/σ_n^2, this provides an array gain equal to M, the number of elements in the array. This performance is degraded when there is directional interference, as this interference might be in the direction of a side lobe.

Null-Steering Beamforming - Zero Forcing

A null-steering beamformer is used to cancel plane waves arriving from known directions and thus produces nulls in the response pattern in the Direction of Arrival (DoA) of the plane wave. This may be done by estimating the weights of a beamformer using suitable constraints. Assume that s0 is the steering vector in the direction where unity response is required and that $\vec{s}_1, \ldots, \vec{s}_k$ are k steering vectors associated with k directions where nulls are required. The desired weight vector is the solution of following simultaneous equations:

$$\vec{w}^H \vec{s}_0 = 1 \tag{3.19}$$

$$\vec{w}^H \vec{s}_i = 0; i = 1, \ldots, k \tag{3.20}$$

Using matrix notation, this becomes

$$\vec{w}^H A = \vec{e}_1^T \tag{3.21}$$

For $k = M - 1$, A is a square matrix. Assuming that the inverse of A exists, which requires that all steering vectors are linearly independent, the solution for the weight vector is given by

$$\vec{w}^H = \vec{e}_1^T A^{-1}. \tag{3.22}$$

In case the steering vectors are not linearly independent, A is not invertible, and its pseudo inverse can be used in its place:

$$\vec{w}^H = \vec{e}_1^T A^H (A A^H)^{-1}. \tag{3.23}$$

Although the beam pattern produced by this beamformer has nulls in the directions of interferences, it is not designed to minimize the uncorrelated noise at the array output.

Optimal Beamforming

The null-steering scheme described above requires knowledge of the directions of interference sources, and the beamformer using the weights estimated by this scheme does not maximize the output SINR. The optimal beamforming method described in this section overcomes these limitations. The algorithm is also known as Minimum Variance Distortionless Response (MVDR) beamformer [15]. For an unconstrained array, the weights that optimize the output SINR are

$$\hat{\vec{w}} = \mu_0 R_N^{-1} \vec{s}_0. \tag{3.24}$$

As noise covariance matrix R_N does not contain any signal from the look direction. For an array constrained to have a unit response in the look direction, the constant μ_0 becomes

$$\mu_0 = \frac{1}{\vec{s}_0^H R_N^{-1} \vec{s}_0} \tag{3.25}$$

This beamformer is also known as the Maximum Likelihood filter, as it finds the Maximum Likelihood (ML) estimate of the power of the signal source, assuming all sources as interferences.
If the noise-alone matrix is not available, the total R (signal plus noise) can be used instead. In the absence of errors, the processor performs identically in both cases. The weights are then

$$\hat{\vec{w}} = \frac{R^{-1}\vec{s}_0}{\vec{s}_0^H R^{-1} \vec{s}_0}. \tag{3.26}$$

These weights are the solution of the following optimization problem:

$$minimize \quad \vec{w}^H R \vec{w} \tag{3.27}$$

$$subject \quad \vec{w}^H \vec{s}_0 = 1. \tag{3.28}$$

Thus, the processor weights are selected by minimizing the mean output power of the processor while maintaining unity response in the look direction. The constraint ensures that the signal passes through the processor undistorted. Therefore, the output signal power is the same as the look-direction source power. The minimization process then minimizes the total noise, including interferences and uncorrelated noise. Minimizing the total output noise while keeping the output signal constant is the same as maximizing the output SNR.
The processor with these weights is referred to as the optimal processor. The output SINR $\hat{\alpha}$ of the optimal processor is given by

$$\hat{\alpha} = p_s \vec{s}_0^H R_N^{-1} \vec{s}_0. \tag{3.29}$$

For the optimal beamformer to operate as described above and to maximize the SINR by canceling interferences, the number of interferences must be less than or equal to $M-2$, as an array with M elements has $M-1$ degrees of freedom (free parameters, possibilities to place nulls or maxima) and one has been utilized by the constraint in the look direction. This may not be true when multipath exists, and the beamformer may not be able to achieve the maximization of the output SINR by suppressing every interference. However, suppressing parts of the interference is still an improvement.

Optimization Using Reference Signal

The optimal beamformer described above needs the knowledge of the direction of the desired signal. This can be substituted by the knowledge of a reference signal. The array output is subtracted from an available reference signal $r(t)$ to generate an error signal $\epsilon(t) = r(t) - \vec{w}^H \vec{x(t)}$, which is used to control the weights. Weights are adjusted such that the Mean Squared Error (MSE) between the array output and the reference signal is minimized. The MSE is given by

$$MSE = E[|\epsilon(t)|^2] = E[|r(t)|^2] + \vec{w}^H R \vec{w} - 2\vec{w}^H \vec{z} \tag{3.30}$$

where $\vec{z} = E[\vec{x}(t) r(t)]$ is the correlation between the reference signal and the array signal vector $\vec{x(t)}$. The MSE surface is a quadratic function of $\vec{w}$ and is minimized by setting its gradient with respect to $\vec{w}$ equal to zero, yielding the solution

$$\hat{\vec{w}}_{MSE} = R^{-1} \vec{z}. \tag{3.31}$$

The MSE of the processor, also known as the Wiener filter, using these wieghts is given by

$$MMSE = E[|r(t)|^2] - \vec{z}^H R^{-1} \vec{z}. \tag{3.32}$$

The MSE minimization scheme (the Wiener filter) is a closed-loop method compared to the open-loop scheme of MVDR (the ML filter) described in the previous section. In general, the Wiener filter provides higher output SINR compared to the ML filter in the presence of a weak signal source. As the input signal power becomes large compared to the background noise, the two processors give almost the same results. The increased SINR by the Wiener filter is achieved at the cost of signal distortion caused by the filter. The required reference signal for the Wiener filter may be generated in a number of ways. A synchronisation signal, e.g., the preamble may be used for initial weight estimation, followed by the use of the detected signal as reference signal. A user specific sequence might also be used.

3.1.2.4 Algorithm Selection

In most deployments, only BSs have antenna arrays because antenna arrays are too big and too costly for (mobile) SSs. This avoids the usage of spatial multiplexing techniques, since they require multiple antennas at both nodes. Beamforming performs well for high element or channel correlation, whereas diversity coding and spatial multiplexing are interesting in low element/channel correlation environments [7]. Highly correlated transmission channels can be found in rural and suburban scenarios, especially with LOS or

over-the-rooftop antennas. Due to the multipath environment, channels tend to be uncorrelated in urban scenarios. The optimal beamforming algorithm has been implemented in the simulation environment. As described in Section 3.1.2.3, the optimal beamformer calculates a beam pattern that realizes a gain of one in the direction of the desired SS. As the algorithm minimizes the total radiated energy, it reduces the antenna gain towards undesired SSs. Figure 3.2 shows the beam patterns for a three SS environment. The size of the side lobes can be influenced by assuming a different noise level when building the array correlation matrix. Figure 3.2 shows three exemplary beam patterns for a 9-element Uniform Linear Array (ULA) and Uniform Circular Array (UCA). The difference is in the position of the antenna elements. In a ULA they are aligned in a line. As Figure 3.2(a) shows, the ULA array allows thin beam widths but has the disadvantage of always exhibiting a symmetry with respect to the array's axis. Thus, ULAs are usually used in sectorized deployments where only one sector is served by the array. In contrast, the UCA shown in Figure 3.2(b) features slightly wider beams but is better suited for the deployment at the base station of an unsectorized cell.

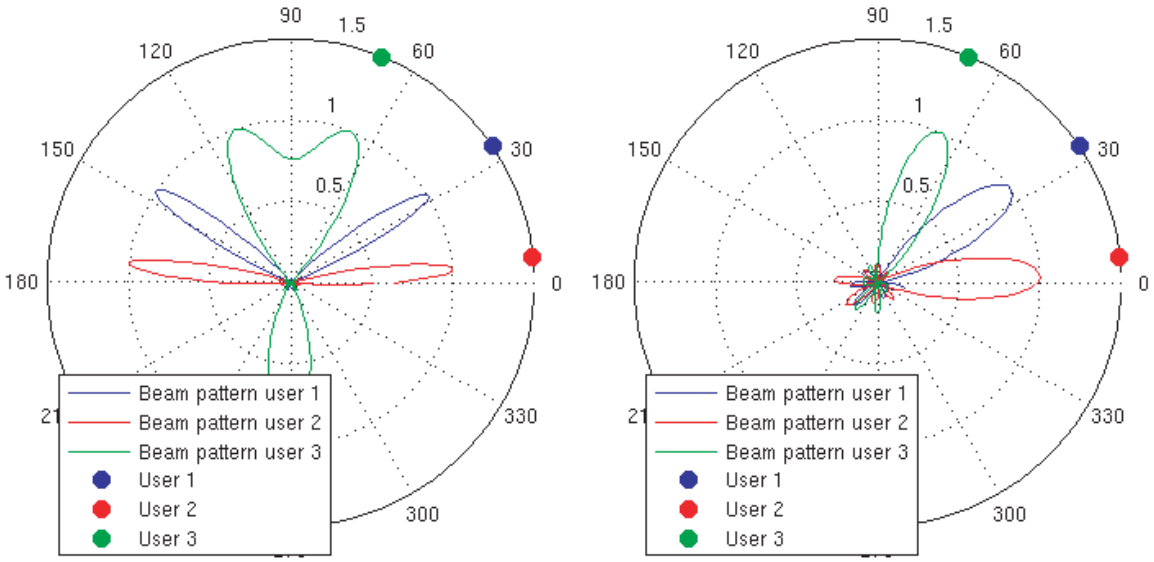

(a) ULA (b) UCA

Figure 3.2: Radiation patterns for 9-element circular and linear antenna arrays

3.1.3 SDMA[18]

The term SDMA denotes the possibility for multiple, spatially separable SSs to access the medium at the same time, on the same frequency. This can be realized using a beamforming system. The linear nature of an antenna allows a superposition of several signals onto one antenna element. If the beam patterns (resulting from the corresponding weight vectors w_1 ,w_2, ..., w_N) have high gains in the direction of the desired SSs and low gains in the directions of concurrent, undesired SSs, each station will receive its signal with a sufficient SINR. An example SDMA transmission to three SSs is given in Figure 3.2: SS 1, SS 2 and SS 3 can be served simultaneously because each SS's pattern has a null set in the other SS's direction. In the uplink, when SS 1, 2 and 3 concurrently transmit to the beamforming station, joint detection techniques of the beamforming system allow the parallel reception. This can be seen as setting "receive beam patterns".

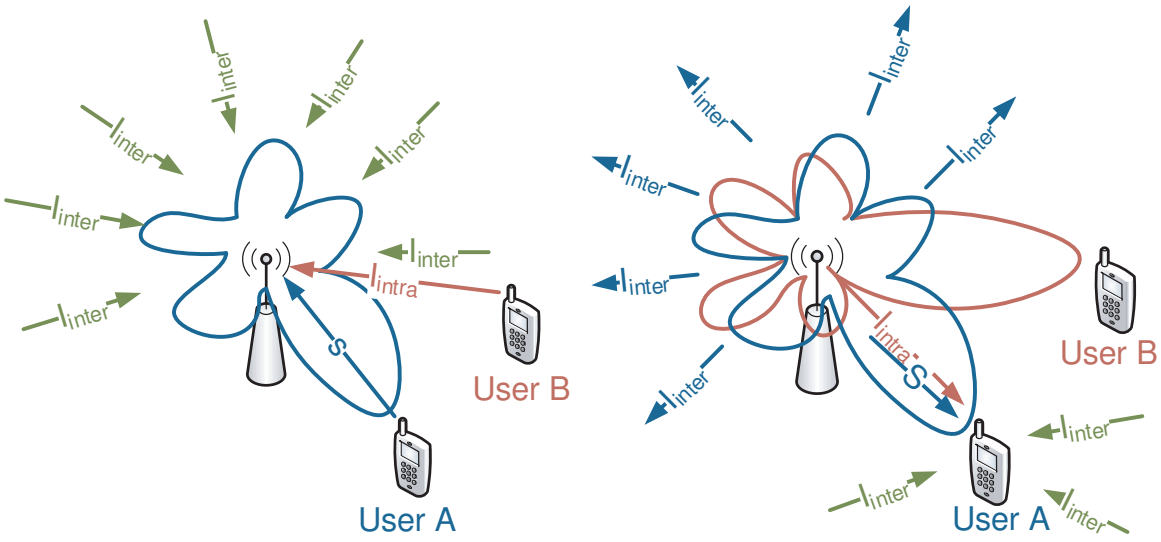

(a) Rx (b) Tx

Figure 3.3: Relevant signals during SDMA

3.2 SINR estimation for SDMA[18]

The SINR of a user or a BS during reception is defined as the ratio of the received signal and the addition of the interference signals and receiver's thermal noise:

$$SINR[dB] = 10 \cdot log_{10}\left(\frac{Carrier[W]}{Interference[W] + Noise[W]}\right) \tag{3.33}$$

When a BS transmits using an omnidirectional antenna, if it knows the pathloss, the (inter-cell) interference, and the noise level at the user, it can estimate the user's SINR. Usually, the BS knows the pathloss to the user. Moreover, if the BS knows the user's transmit power it can do the same calculation using the signal strength received from the user. In any case, values of the interference level experienced by the user have to be explicitly signaled or have to be estimated.
Figure 3.3(a) shows the relevant signals during concurrent SDMA reception data from spatially separated users. An optimized antenna pattern is applied at the BS. It maximizes the desired signal S from user A and minimizes the intra-cell interference I_{intra} from user B, which is concurrently transmitting. All intra-cell interferers have to be counted as well. The third component of the received signal power is generated by neighboring co-channel cells I_{inter}. By minimizing the side-lobes of the beam patterns, the beamforming algorithm can try to minimize the base station's exposure to inter-cell interference. The SINR estimation for SDMA reception has to consider all signals metioned above. All these signals are filtered through the optimized pattern, denoted by the superscript ^{opt}. Finally, the receiver noise at the BS N has to be taken into account. The result is given by

$$SINR_{Rx} = \frac{S^{opt}}{N + I_{inter}^{opt} + \sum_{SDMAusers} I_{intra}^{opt}} \tag{3.34}$$

Figure 3.3(b) shows the relevant signals during concurrent SDMA transmission data from spatially separated users. An optimized antenna pattern is applied at the BS. This pattern maximizes the desired signal S to user A. The other patterns that are optimized for concurrent transmission to other users, try to minimize the intra-cell interference I_{intra} to user A. Neighboring cells contribute to inter-cell interference I_{inter} at the receiver. During the transmission, the desired signal S and the intra-cell interference I_{intra} are filtered through the corresponding optimized beam patterns, denoted by the superscript ^{opt}. Assumed that the user is receiving omnidirectionally, the inter-cell interference is not filtered. By reducing the side-lobes of the BS's antenna patterns the inter-cell interference caused in neighbor cells can be minimized. Finally the receiver noise N at the SS has to be considered as well. The result is given by

$$SINR_{Tx} = \frac{S^{opt}}{N + I_{inter} + \sum_{SDMAusers} I_{intra}^{opt}} \tag{3.35}$$

The PHY-module used in the simulations provides SINR estimation facilities based on the considerations given above. In a real-world base station, these values would most probably be based on measurements signaled back by user stations and on approximate estimations for the intra-cell interference. Alternatively, the weight vectors computed from the received signals could be used to reconstruct the beam patterns from which the relevant gain entries could be retrieved[12].

3.3 SDMA Scheduling[18]

Time Division Multiple Access (TDMA) systems can arbitrarily assign different SSs to diferent time slots because time slots are orthogonal as they do not overlap. Usually they are even separated by guard times. Thus, mutual interference for SSs assigned to distinct TDMA slots can be ruled out. The dimension time can be considered as being nearly perfectly orthogonal. Using other multiple acces schemes, such as Frequency Division Multiple Access (FDMA) or Code Divison Multiple Access (CDMA), SSs are scheduled onto different frequency (sub-) bands or orthogonal spreading codes are assigned to different SSs. Thus, channel assignments in the frequency or code domain can be considered nearly orthogonal, too. For the spatial dimension, the picture is different. Even though the number of antenna elements limits de spatial dimension, modeling TDMA-SDMA resources as a two-dimensional cube with orthogonal access is not suitable. SSs cannot be arbitrarily scheduled for parallel SDMA transmissions at the same time beacuse there is spatial separability by the beamforming antenna array depends on their relative spatial positions. To overcome this problem, a hierarchical scheduling approach is introduced in the following that first computes a spatial grouping of SSs that can be well separated by the BSs beamforming antenna. The result of this grouping is a set of spatial groups of SSs. SSs of the same group can be separated and thus be served at the same time. SSs from different groups are not spatially separable so that SSs of different groups have to be separated in the time domain. Consequently, the spatial groups are scheduled using conventional secheduling methods. The separation of the scheduling process into two hierarchical stages, additionally adds flexibility and simplicity to the scheduling process. The grouping process is independent from the TDMA scheduling and viceversa. Thus,

spatial grouping and group scheduling procedures can be combined and interchanged freely in accordance with the specific needs of the target system.

3.3.1 Spatial Grouping

As introduced above, the first step in the combined TDMA-SDMA scheduling process is a spatial grouping process that partitions the set of SSs into groups of SSs. The SSs of a group are well separable by the beamforming antenna and can therefore be co-scheduled for the same TDMA resource. This section first defines the characteristics of such a grouping. Second a metric to compare the performance of differente grouping is introduced. Finally, the grouping algorithm used is presented.

3.3.1.1 Definition of a Spatial Grouping

In mathematical terms, a spatial grouping is a partition $\mathcal{P} = \{G_1, G_2, \dots\}$ of the set of all SSs U. Every SS $u_i \in U$ belongs to exactly one spatial group $G_j \subseteq U$. A combination of groups has to fulfill the two conditions defining a partition:

1. all groups have to be mutually exclusive, i.e., no SS can be in more than one group
2. the groups have to be collectively exhaustive, i.e, every SS from the set of all SSs has to be covered by a group

In a scheduler, not every partition is allowed as a valid grouping. On the one hand, the smart antenna system supports only a limited number of concurrent beamforming transmissions. If the maximum number of supported beams is denoted by k, only partitions $\mathcal{P}$ whose subsets G_j have cardinalities that are limited by k, i.e., $|G_j| \leq k \quad \forall G_j \in \mathcal{P}$ are allowed. On the other hand, a partition is invalid if it leaves a SS unserved. This might occur when SSs that are not well separable are grouped together. In this case, the mutual interference might become such high that one or several SSs perceive an SINR that is not sufficient for successful decoding. Considering such a grouping would contradict the objective to achieve high system throughput while serving all SSs.

3.3.1.2 A Performance Metric for Spatial Groupings

In order to be able to compare different groupings and to choose "the best" grouping, a metric that assigns a quantitative value to a grouping is necessary. In the end, utilizing SDMA should increase the system throughput compared to the non-SDMA, i.e., the TDMA case. Therefore, a metric should use the achievable throughput capacity (gain) relative to the non-SDMA case as the central performance measure.
Grouping SSs into one group that fits into a TDMA slot, which would otherwise be occupied by only a single SS, seems to increase the possible throughput in that time slot. However, the grouping comes at a cost: The SSs' SINR will suffer when they are co-scheduled with other group members. Depending on the decrease in SINR and the link adaptation of the specific system, a reduced SINR value might lead to a lower data rate for the SS.
The proposed grouping metric considers both effects. Equation 3.36 defines the throughput gain of a spatial grouping

$$gain = \frac{\sum_{i=1}^{n} Throughput_{SDMA}(u_i)}{\sum_{i=1}^{n} Throughput_{NON-SDMA}(u_i)} \frac{U}{\mathcal{P}} \tag{3.36}$$

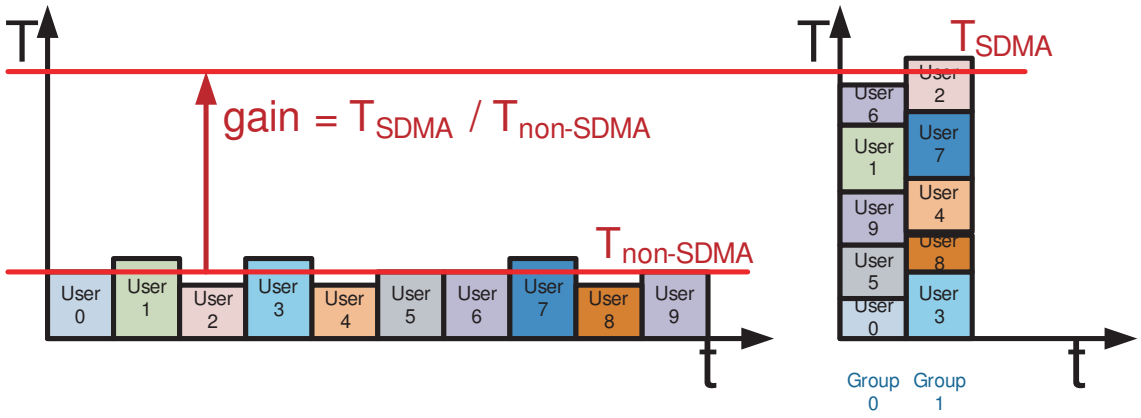

Figure 3.4: Example SDMA throughput (T) gain realized by grouping 10 SSs into 2 groups

that might be lower than 1.0. The gain is the ratio between the number of SSs $|U| = n$ and the number of groups $|\mathcal{P}|$ in a grouping $\mathcal{P}$ where instead of $|U| = n$ only $\mathcal{P}$ time slots are needed to carry the traffic of a saturated system.
Figure 3.4 shows an exemplary grouping of 10 SSs into 2 groups. Even though some groups experience slightly lower throughput rates ($T_{SDMA} \leq T_{NON-SDMA}$), a gain appears possible to be achieved because only 2 instead of 10 time slots are needed to carry the same amount of data.

3.3.2 Grouping Algorithm

In this thesis the grouping algorithm used is the tree-based grouping heuristics, following introduced.

3.3.2.1 Tree-based Grouping Heuristic

The tree-based grouping algorithm constructs its groupings as levels of a tree. It starts with a grouping that serves each SS in its own group. This trivial grouping forms the first level of the tree. From there, the algorithm builds higher levels by joining two groups. The criterion to select the two groups can be chosen arbitrarily in the form of a utility function that reflects how much the grouping can benefit from merging two groups. If this utility function is simply the evaluation of the new group's SINRs then the grouping algorithm can determine an accurate estimate of the achieved gain by mapping the SINRs to throughputs. But it is also possible to use other utility functions that do not perform SINR calculations. For the remainder of this subsection, a SINR based utility function is assumed.
Figure 3.5 shows an example tree that groups a set of five SSs $U = 1, 2, 3, 4, 5$. On the lowest level (tree level 1), all SSs form separate groups. Then, all $\binom{5}{2}$ combinations to join two groups are evaluated and the union with the highest utility is chosen, {1,2} in this example. The resulting grouping forms level 2. At this level, $\binom{4}{2}$ choices are possible and SSs 3 and 4 are joined next. Finally, from level 3 to level 4 only three choices remain and the union {1,2,5} delivering the highest utility chosen. The grouping ends here beacuse the group size limit is three and no more groups could be joined to form a valid grouping. As a last step, all groupings corresponding to the tree levels are evaluated and the grouping with the highest grouping gain is chosen.

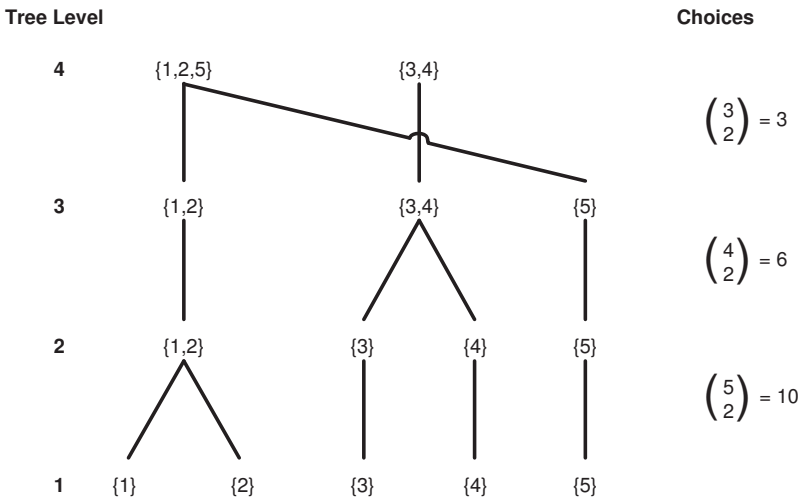

Figure 3.5: Tree-based grouping of a 5-SS set into groups ≤ 3 [14]

(Complexity analysis in [18, p. 101])

3.3.3 TDMA Scheduling of Spatial Groups

This section focuses on the second step in the combined TDMA-SDMA scheduling proces, how the spatial groups are assigned to TDMA slots.
In a packet oriented system, the task of the packet scheduler is to decide into which frame and at which position in a frame a data packet is placed for transmission.
The scheduling strategies used in this thesis are following introduced.

3.3.3.1 Round Robin

Round Robin (RR) serves SSs in frame based rounds. Because all SSs of the current round are given the chance to transmit before the next round starts a new, RR inherently assures a certain degree of fairness. While RR is widely known, there exist many different definitions and variants of it. Here, we will assume that the spatial groups of SSs are given equal time burst lengths during a frame.
Assuming a queueing model (Figure 3.6) and a spatial grouper the scheduler determines the time length of the frame it has to fill and divides it by the number of groups it has retrieved from the grouper to determine the length of each burst. Each group is assigned to one of the bursts and the burst are filled with the SS's data packets.
Every SS that is served in SDMA is assigned a beamforming transmitter unit that transmits its data with a beam that is optimized for it. The spatial grouper computes the optimal beamforming weight vector of each SS and also provides an SINR estimation. Based on this SINR estimation the scheduler can select a Modulation and Coding Scheme (MCS). With the associated data rate, the transmission duration of each packet is known so that the scheduler is able to determine the last packet that fits into the group's burst.

3.3.3.2 Proportional Fair

The Proportional Fair (PF) scheduling strategy aims at a tradeoff between fairness and throughput. The throughput optimization is realized by preferring groups of SSs for which the grouper has estimated high SINR values, thus promising high throughput.

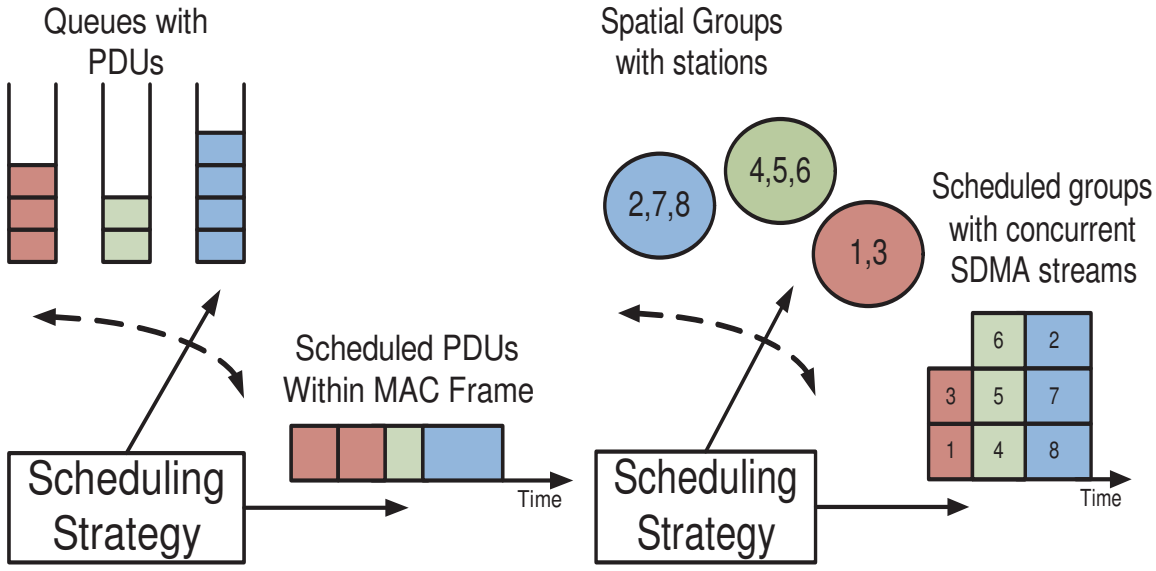

(a) Packet Scheduler (b) Group Scheduler

Figure 3.6: Schematic view on classical packet and hierarchical group scheduler

The fairness is achieved by considering the past data rate that a SSs has experienced. This way, not only groups that promise high throughput in the future, but also those that have experienced throughput below average in the past, are taken into account by the scheduling decision.
The actual importance of a user in view of the scheduler is defined by the ratio of its future and past data rates. The future data rate of a group is easily derived from the estimated data rates of the group members. Determining the past data rate is more difficult. The reason is that groupings may change on a frame-by-frame basis. Therefore, the members of a current group may have belonged to a different group in the past. When choosing members' past data rates as a criterion, high data rate SSs might starve SSs with low data rates. Therefore, the group's total future throughput and the minimum past group member throughput was taken for computing the groups importance in the view of the scheduler

$$importance(G_j) = \frac{\sum_{u \in G_j} EstimatedRate(u)}{1 + \beta min_{u \in G_j}\{PastRate(u)\}} \tag{3.37}$$

This ratio is computed for every spatial group G_j obtained from the grouper. The groups are then served in order of descending importance. The factor β determines how much influence the past data rates have on the group's importance. The algorithm implemented in the WiMAX MAC simulator (WiMAC) takes the past data rates into account using an exponential smoothing, thus reducing the weight of the preceding frames the more the larger the past time value is

$$PastRate_t = \alpha CurrentRate + (1 - \alpha) PastRate_{t-1} \quad 0 \leq \alpha \leq 1 \tag{3.38}$$

In order to avoid intra-group inefficient use of the spatial channels, the PF algorithm has been implemented to finish a group's burst duration once the first group member has run out backlogged packets.

CHAPTER 4

Coordination Across Base Stations

The target of this master thesis is to mitigate the inter-cell interference and to improve its estimation in SDMA enhanced systems by coordination. In order to achieve the target, coordination schemes are presented in which BSs mutually exchange information. The position of their SSs and the point in time when they are allocated is forwarding. In this manner a BS is enabled to improve its SINR estimation by knowing the interferers and to possibly consider inter-cell interferers in the beamforming algorithm. In a Constant Bit Rate (CBR) traffic scenario the future active SSs are known by the serving BS, therefore BSs can simply exchange their early made scheduling decisions. In a Variable Bit Rate (VBR) traffic scenario is not possible to know the future active SSs, thus the coordination strategy has to be completly different to he one in the CBR traffic scenario. The target of this coordination concept is to convert the variable interfering traffic in constant traffic by introducing regions, in order to make the inter-cell interference more predictable. In this chapter, both concepts are introduced.

4.1 Coordination in a Constant Bit Rate Traffic Scenario

In the CBR traffic scenario, SSs have a CBR traffic in DL and UL, and hence have a constant traffic load in every frame. If the SSs have a static position, using the Round Robin scheduling strategy [section 3.3.3.1], the MAC frames remains constant. Therefore, knowledging one frame of the interfering cells is sufficient to know their next frames, and interfering stations can be considered in the interference estimation. If the SSs are mobile, the SDMA groups can differ and therefore the frames can change. Thus, a periodic update of the coordination information is required.

4.1.1 Uplink

In a multicell system, in UL, a receiving SDMA enhanced BS suffers from intra-cell and inter-cell interfering SSs. This approach targets to mitigate inter-cell interference by directing zeros towards interferers. A zero towards one interferer is not possible for example if the interferer is in the direction of the main lobe. In this case at least the interfering station should be known. Hence the approach promises to significantly improve the interference estimation.
The inter-cell power received at the BS can be estimated by knowing the position, the power and the time of transmission of each inter-cell interferer. Table 4.1 shows the Station Information of one burst. It comprises information about the transmitter of the burst: its identity, identity of the BS associated with it, its position, start and end time of transmission, Tx antenna pattern, Tx power and subband. The coordination message comprises the Station Information for all the transmitted bursts.
With the position, the BS is able to estimate the path loss and the Rx and Tx antenna gain. In order to know the position of a SS in its cell, if no Global Positioning System (GPS) signal is availabe, the BS needs to know the DoA and the distance to the SS. With the

Element	Note
idSS	Identity of the interfering SS
idBS	Identity of the BS associated with the SS
Position	Position of the interfering SS in a defined coordinate system
Burst Start Time	Start time of the burst respect the start time of the UL subframe
Burst End Time	End time of the burst respect the start time of the UL subframe
Antenna Pattern	Antenna pattern used for the burst
Tx Power	Power used to transmitt the burst
Subband	Subband used to transmitt the burst

Table 4.1: Station Information for UL

algorihms like ESPRIT, MUSIC or SAGE, the BSs can extract the DoA of each SS [18]. With the SS's signal strength at the BS, the distance between them is known.
Thus, with the information received, the BS estimates the inter-cell interference of each inter-cell SS using the Equation 4.1

$$I_{inter}[dBm] = Power + G_{RXAntenna} + G_{TXAntenna} - PathLoss_{BS-SS} \tag{4.1}$$

Scheduling information is exchanged just before the start of each frame. In order to decouple the coordination process, BSs are sorted in classes as shown in Figure 4.1. Without decoupling the scheduling of a BS at one end of a system would depend on the scheduling of the BS at the other end of the system. Figure 4.2 shows the message sequence chart for the example of coordination with three classes. A BS forwards its secheduling decision not every frame but every third frame, commonly with BSs of the same class.

In a SDMA enhanced system, beam patterns have gains in the direction of the desired SSs and zeros in the directions of undesired SSs (intra-cell interferings).
Besides the new interference estimation, with the information obtained in the coordination, the beam patterns have low gains in the directions of inter-cell interferings as well. Figure 4.3 shows the new beamforming strategy, using the inter-cell and intra-cell interfering stations as undesired stations in the beamforming algorithm.

A new burst is built for every different set of interferers because for each different set of interferers a new beam pattern has to be employed. Figure 4.4 despicts an example UL subframes of BS2, BS3 and interfered BS1. The Group9 of BS1 has three different set of interferers: Group1 and Group5, Group2 and Group5, and Group2 and Group6. The one burst of Group9 is divided three bursts. Three different patterns are applied directing zeros to the different interferers in each burst of burst of Group9. This concept of coordination is named *Direct zeros towards inter-cell users*.

4.1.2 Downlink

The approach in DL is similar to the UL case. In DL single antenna SSs receive inter-cell inteference from neighbor BSs. The inter-cell interference is mitigated by directing zeros at the neighbor BS towards the interfered SSs.

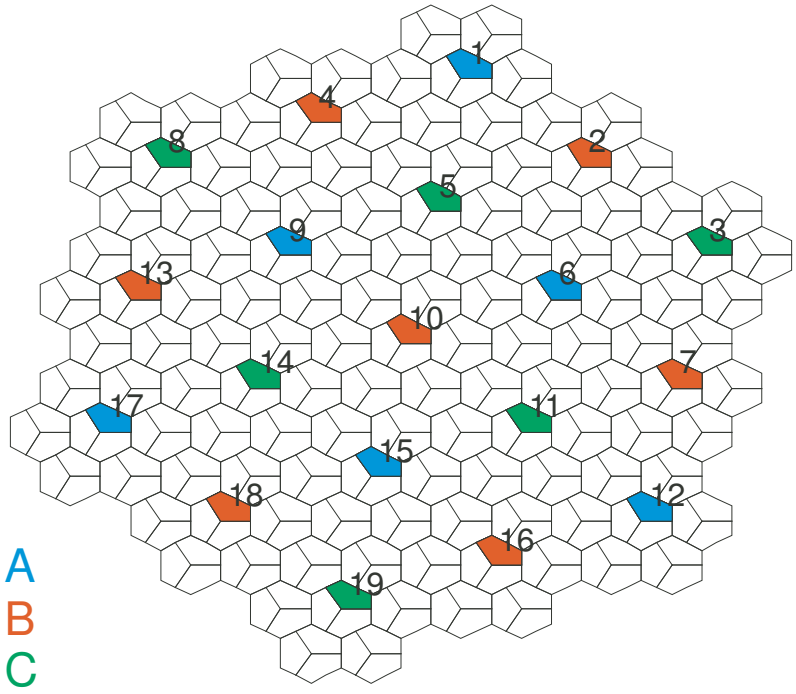

Figure 4.1: BS classification

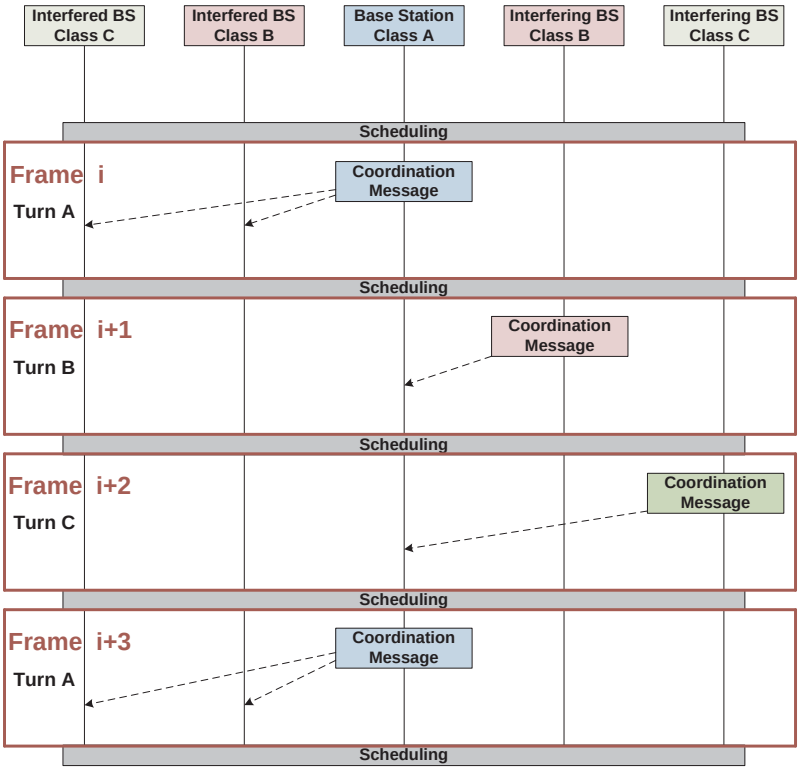

Figure 4.2: Message sequence chart(UL)

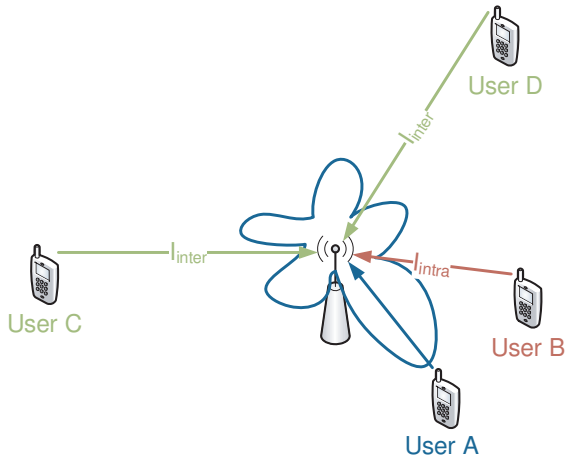

Figure 4.3: Antenna pattern with intra and inter-cell interferings

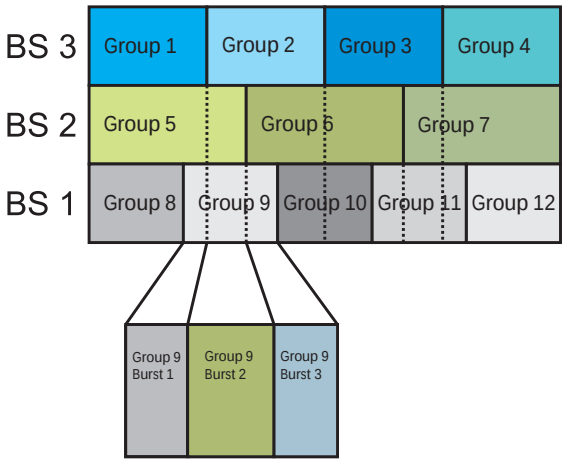

Figure 4.4: UL Subframes. BS 2 and BS 3 interfere BS1. New burst with new beam pattern for each different set of interferers

Element	Note
idSS	Identity of the receiver SS
idBS	Identity of the interfering BS
Position	Position of the interfering BS in a defined coordinate system
Burst Start Time	Start time of the burst respect the start time of the DL subframe
Burst End Time	End time of the burst respect the start time of the DL subframe
Antenna Pattern	Antenna pattern used for the burst
Tx Power	Power used to transmitt the burst
Subband	Subband used to transmitt the burst

Table 4.2: Station Information for DL (towards interfered cells)

Element	Note
idSS	Identity of the interfered receiver SS
idBS	Identity of the BS associated with the SS
Position	Position of the interfered SS in a defined coordinate system
Burst Start Time	Start time of the burst respect the start time of the DL subframe
Burst End Time	End time of the burst respect the start time of the DL subframe
Subband	Subband used to transmitt the burst

Table 4.3: Station Information for DL (towards interfering cells)

Calculating the inter-cell interference requires to know the position, the power and the time of transmission of each inter-cell interferer.
The BS sends a coordination message to their interfering BSs. This comprises the Station Information of all bursts. Thus, the interfering BSs are able to direct zeros towards the interfered stations. After receiving the coordination message from the interfering BSs including the antenna pattern, the BS of the interfered cell calculates a new SINR estimation in the interfered SSs.
Tables 4.2 and 4.3 show the Station Information of one burst. The Table 4.2 show the Station Information to send towards an interfered cell. The Table 4.3 show the Station Information to send towards an interfering cell.
The BSs are classified as in UL Figure 4.5 shows the message sequence chart for the example of coordination with three classes. A BS forwards its secheduling decision not every frame but every third frame, commonly with BSs of the same class.

A new burst is built for every different set of interfered stations or interfering stations' beam pattern.

4.1.3 Alternative design: One burst per group

As mentioned above, *direct zeros towards inter-cell users coordination* modifies the Round Robin algorithm in order to create a burst for each set of interfering/interfered stations. If the number of groups in the interfering/interfered cells is high and different, the number of burst per group is highly increased and their duration decreases. Therefore, depending on the packet size used and the MCS selected, these small burst could not be filled by data.
In order to avoid this problem, a modification of *direct zeros towards inter-cell users coordi-*

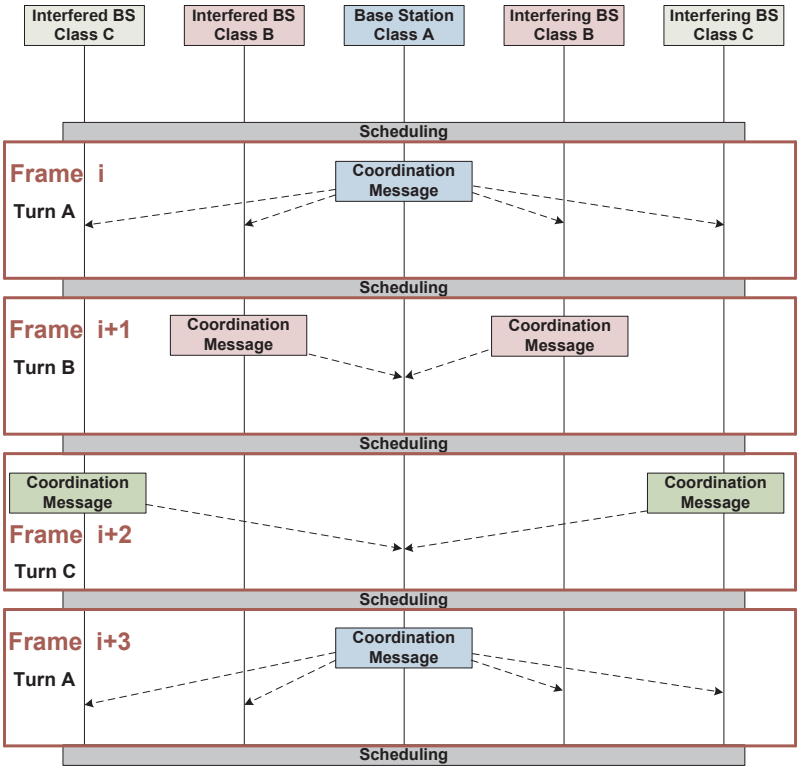

Figure 4.5: Message sequence chart (DL)

nation is designed: *direct zeros towards inter-cell users (one burst per group) coordination*. In this approach, the Round Robin algorithm is not modified: one burst per group.
The antenna pattern and the SINR estimation is unique for the whole burst. All the interfering/interfered stations of the burst have to be considered in the beamforming algorithm and SINR estimation for the whole burst.

4.2 Coordination in a Variable Bit Rate Traffic Scenario

With VBR traffic, a BS has a randomly different traffic load in every frame in DL and UL. Hence a BS cannot schedule a frame early before the frame transmission and forward its scheduling decision to neighbor BSs. Therefore, the coordination approach CBR scenario cannot be applied on the VBR case.
In order to allow for reliable prediction of the traffic load and its interference, in the following approach SSs are grouped into spatial regions. The traffic upcome and the interference of this spatial regions are then assumed as constant.
The following coordination concept is called *Spatial regions*.

4.2.1 Uplink

In this coordination method the sectors are divided into spatial regions. Each BS defines the spatial regions of its interfering cells. The spatial regions have the same size in order to have the same potential number of stations.
At anytime only one SS of each region can transmit, thus the regions are perceived as one SS. The sources of inter-cell interference can be estimated as a fixed number of SSs. If the

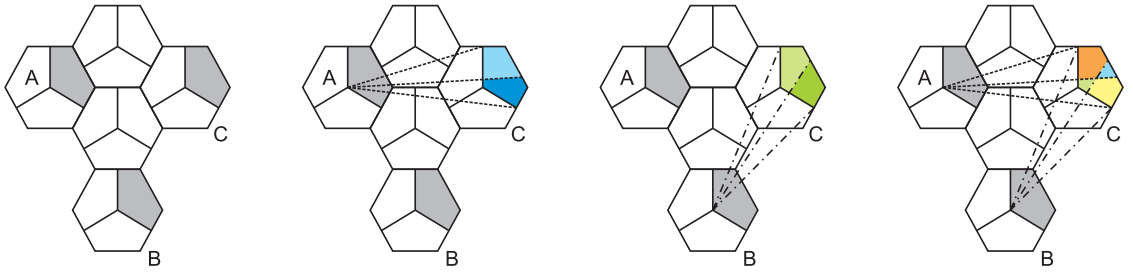

(a) Cluster order 3 scenario

(b) Regions in BSC due to BSA

(c) Regions in BSC due to BSB

(d) Subregions in BSC due to BSA and BSB

Figure 4.6: Creation of spatial regions and subregions. Basis: two interfered BS and two concurrent antenna beams

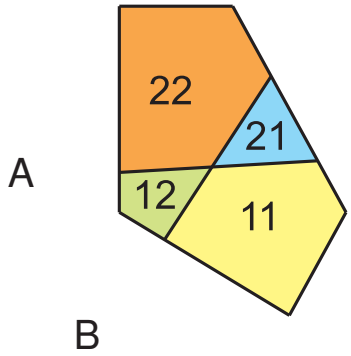

Figure 4.7: Spatial subregions. Basis: two interfered BSs and two concurrent antenna beams

SSs of regions have enough traffic to transmit anytime, the traffic of the regions becomes a CBR traffic, and the inter-cell interference as well.
Because the idea is to have only one SS per region concurrently transmitting, the number of regions is the same as the maximum number of concurrent beams.

When a BS has more than one interfered BS, subregions are created by the superposition of regions belonging to the different interfered BSs. The Figures 4.6 show how the spatial regions and subregions are built.
Each subregion is coded by a number, and each digit of that *subregion number* indicates in which region of one interfered BS the BS is situated. Thus, there are as many digits as interfered BSs [refer to Figure 4.7]. In the example of Figure 4.7, if one SS is inside the region 2 of BS A and region 1 of BS B, its *subregion number* is 21.

In order to apply this concept of spatial regions, the SDMA grouper is modified by adding a spatial condition. Ideally, *a SDMA group is valid when it contains one SS of each region*. This condition cannot be always fulfilled, depends on the SSs' position and the number of active SSs. Therefore a relaxed condition is added in the SDMA grouper: *a SDMA group is valid when it contains at most one SS of each region*. In terms of *subregion number*, a group is valid when the digits of the each *subregion number* group member are different. In the example of Figure 4.7, valid groups can be built with SSs of subregions 11 and 22 or 12 and 21.

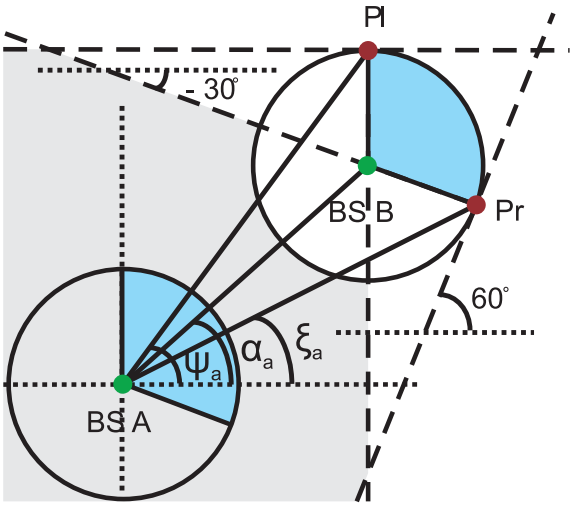

Figure 4.8: Angular constrains

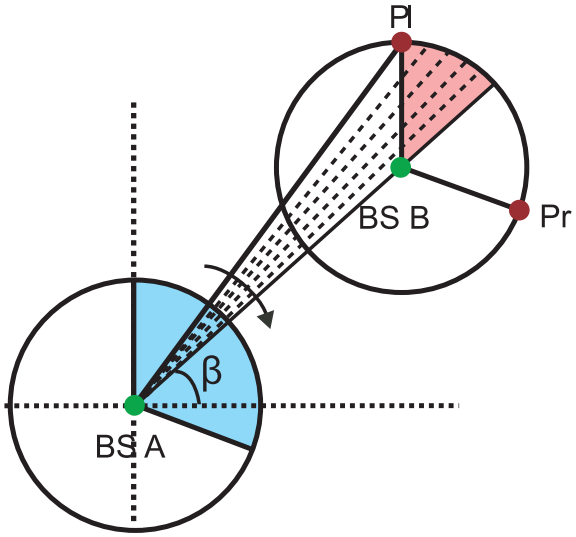

Figure 4.9: Iterations in order to find the angles of the regions

As explained above, the spatial regions of one cell depend on the interfered BSs. The relative position between both BSs determines the regions shape. The algorithm creating the regions and determining the virtual Spatial Super User (SSU)s' position, cells are considered as circles with three sectors. The relative position between the two BSs has to fulfill the following constrains:

1. α_a (angle between interfering BS and interfered BS) $\leq 90°$
2. α_a (angle between interfering BS and interfered BS) $\geq -30°$
3. ψ_a (angle between left point (Pl) and interfered BS) $\geq 0°$
4. ξ_a (angle between right point (Pr) and interfered BS) $\leq 60°$

Figure 4.9 shows how the regions of same size are created.
Angle β is decreased until the seperated area has the desired size, i.e., sector size divided by the number of regions. The found angle is saved as the border of the first region.

In order to mitigate and estimate the inter-cell interference of the regions, a virtual

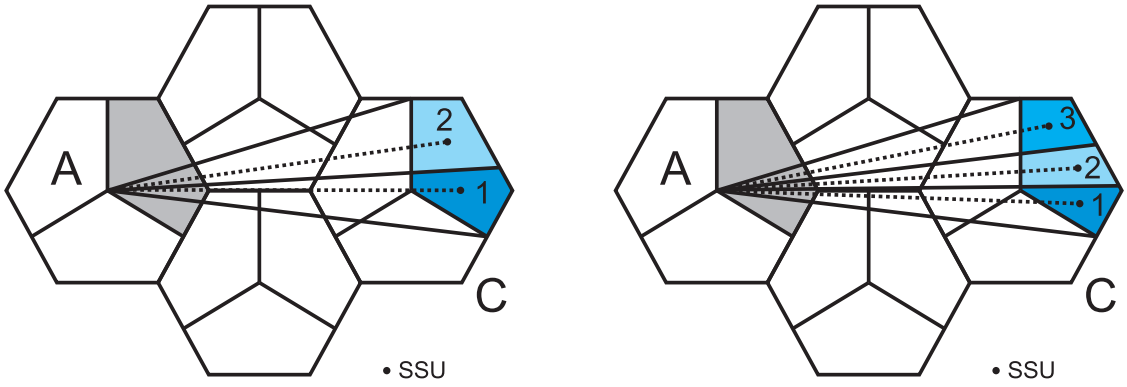

(a) 2 Regions Scenario (b) 3 Regions Scenario

Figure 4.10: Position of the SSUs

SSU is built for each region. The SSUs are modelled as normal SSs and are situated at the weight point of each region, from the point of view of the interfered BS.

Further information about the regions and virtual SSU can be found in Appendix A.

The BSs directs zeros towards the direction of the SSUs of their interfering regions. The position of the SSU and the angular width of the regions determines how good and reliable is the zero of the beam pattern. Figures 4.10 show an aproximation of how the SSUs are situated in the regions. With a higher number of regions, the angular widths are smaller, therefore the estimation is better and the zeros in the antenna beam pattern are more effective.

The interfered BS uses this SSU estimating the average inter-cell interference strength of that region instead of using the specific SS. The inter-cell interference estimation at the interfered BS from a SSU is calculated by equation 4.2.1.

$$I_{inter}[dBm] = Power + G_{RXAntenna} + G_{TXAntenna} - PathLoss_{BS-SSU} \tag{4.2}$$

The total inter-cell interference at the BSs is estimated as the addition of the interference generates by its virtual SSUs.

4.2.2 Downlink

In DL the virtual SSU are used in order to mitigate the inter-cell interference, but the spatial condition is not added to the SDMA grouper, thus the stations are not grouped into spatial groups. These virtual SSU are the same as in UL.

CHAPTER 5

Implementation

This chapter describes how the concepts introduced in chapter 4 are implemented in the open Wireless Network Simulator (openWNS). First, the openWNS is briefly introduced.

5.1 open Wireless Network Simulator

The openWNS developed at ComNets is a simulator that allows the simulative performance evaluation of mobile radio networks (IEEE 802.16, IEEE 802.11, UMTS and the WINNER Protocol Stack). Its concept is to provide a complete protocol stack from the application layer down to the physical layer and radio channel in order to make simulations as realistic as possible. The different layers are offered as modules, and they can easly be exchanged [11] [10].
OpenWNS comprises modules for the following categories:

- Load generators
- Transportation
- Network
- Radio Access Technology (including MAC, RLC, RRM funtionalities)
- Interference Calculation

The simulator finally consists of one or more modules being loaded at runtime by the runtime environment. As mentioned above, each module has a specific task and roughly fits into one of the five categories. To enable the fast and reliable development of new modules supporting the performance evaluation of wireless networks, openWNS provides a set of support libraries. The set of support parts includes:

SPEETCL - SDL Performance Evaluation Tool Class Library A library being used by all simulators that are implemented in the Specification and Description Language (SDL). SPEETCL functionality currently in use by non-SDL simulators is the event scheduler, probes, random number generation, distributions and basic data types for communication protocols.

libWNS - the openWNS support library Among others, it features the following functionalities:

- Module handling support.
- Logging system.
- Configuration facilities.
- Decorators for SPEETCL mechanisms including probes, probability distributions and event queuing.
- Template based containers, extending those available in STL.

RISE - Radio Interference Simulation Engine A library for the simulation of radio interference. It provides the following models:

- Stations (base, relay, mobile).
- Transmitter and receiver.
- Transmission behavior.
- Propagation including shadowing and fading.

- Interference calculation.
- Mobility.
- Antennas.

In this thesis the modified modules and libraries are list below:

1. *WiMAC* (radio access technology)
2. *OFDMA Phy* (interference calculation)
3. *Constanze* (load generator)
4. *libWNS*
5. *RISE*

5.1.1 Event-Driven Simulation

The openWNS is an event-driven simulator, the state of the whole system is changed by a discrete events like transmission or reception of a data packet. These events are organized by a superior timing instance, that keeps track of the simulation time and invokes all necessary subrutines of the different modules at the time at which an event occurs [11].

5.1.2 FUN

A protocol within one ISO/OSI layer has many functionalities. These functionalities are represented by Functional Unit (FU)s which are the implementation of the different parts of a layer within the openWNS. All the FUs of a layer create a FUN. Thus a FUN is the inside view of a openWNS OSI layer with each FU implementing one aspect of the whole protocol[11].

5.2 Implementation

5.2.1 Network coordinator

Task

The `Network Coordinator` class handles the three coordination concepts defined in chapter 4.

Description

This new class is implemented inside the WiMAC FUN, as member of the Management Plane. The `Network Coordinator` class is defined as a `Singleton Holder` and all the FU of the WiMAC FUN can access it. Figure 5.1 shows the WiMAC FUN, the following FUs call the `Network Coordinator`:

1. `ULMapCollector/DLMapCollector`
2. `ULScheduler/DLScheduler`
3. `PhyUser`

For the coordination approach *zeros towards inter-cell users*, the `Network Coordinator` times the BSs, defines the interfering cells of each BS (in UL and DL) and simulates the exchange of information. In UL the `Network Coordinator` provides the Station Information (of each interferer) (position, start and end time of transmission, Tx power and subband) to the

strategy module. In DL, the `Network Coordinator` provides the Station Information of each interfered and interfering station to the strategy module, and estimates the inter-cell interference.

For *Spatial regions coordination* the `Network Coordinator` class creates the regions and the virtual SSUs, as appendix A explains, and allocates the SSs to regions. In order to avoid the creation of a new type of station, the `Network Coordinator` class searchs the closest SS for each virtual SSU, and uses these SSs as virtual SSUs.

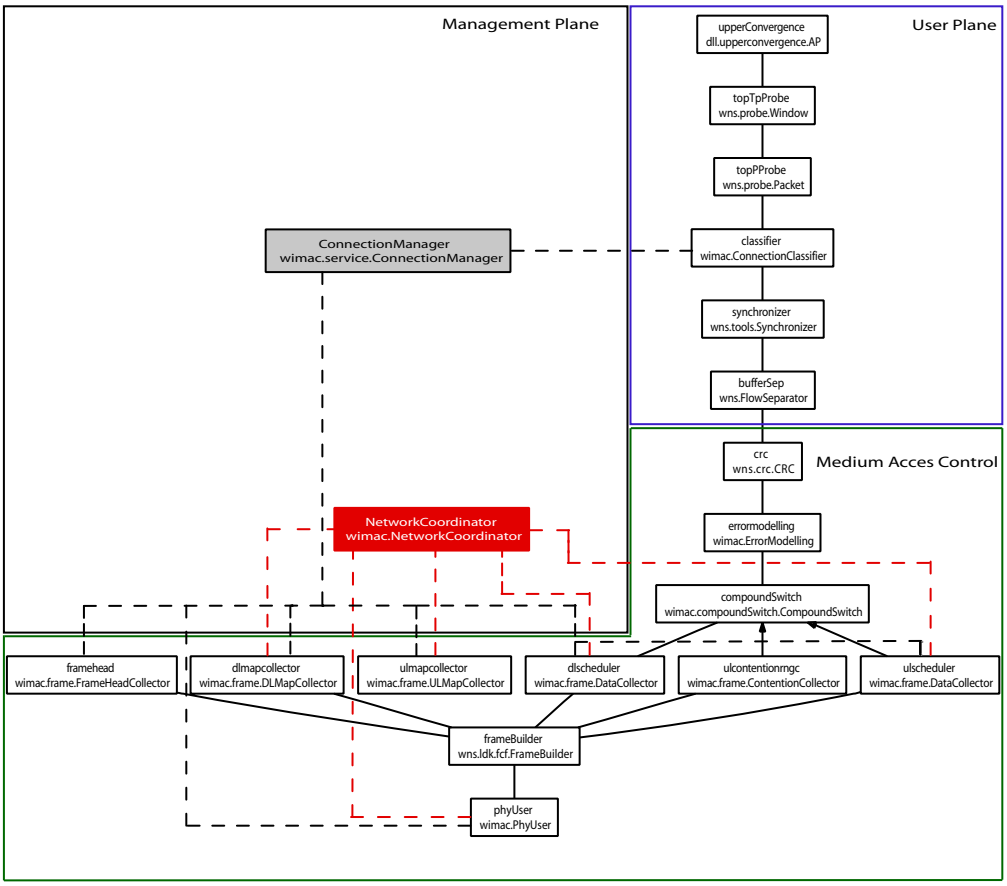

Figure 5.1: WiMAC FUN representing the MAC layer at the BS

5.2.2 Sectorisation for inter-cell interference calculation

Task

Enable sectorisation within the interference calculation, either for UL or DL.

Description

The concept of sectorisation is implementeted within the interference calculation method of the class `Receiver` of `OFDMAPhy` module in order to calculate the inter-cell interference. The added code calculates the angle

between the receiver station and the transmitter, and if the angle is beyond the sector bounds, the transmitter's signal is not added as interference.

5.2.3 Mobility inside sectors

Task

Enable mobility inside a sector.

Description

This modification adds the concept of sectors within the mobility module. The implementation of mobility inside sectors modifies the class `Brown` and the file `mobility.py` of `RISE` library.

5.2.4 Beamforming with inter-cell users

Task

Add the inter-cell interfering (UL) and interfered (DL) users within the beamforming algorithm.

Description

Within the `Beamforming` class of `RISE` library two new methods are implemented. `calculateCandIsRxWithInterCell` method calculates the carrier and interference by directing zeros towards the inter- and intra-cell interfering users. The interference is calculated as the addition of the intra- and inter-cell interference and the `noise`. `calculateCandIsTxWithInterCell` method calculates the carrier and the interference by directing zeros towards the inter-cell interfered users and intra-cell interfering users. The interference is calculated as the addition of the intra-cell interference and the `iIntercellPlusNoise` input. Both methods return the SSs' carrier and interference.

5.2.5 Segmented Round Robin

Task

Modify the conventional Round Robin algorithm, introduced in section 3.3.3.1, in order to create additional bursts and apply the *Zeros towards inter-cell users coordination* concept.

Description

This new strategy with the support of the `Network Coordinator` class modifies the `Round Robin` class, creating a new burst for each set of interferers in UL. For DL, a new burst is built for each different set of interfered SSs or interferers' beam pattern.

5.2.6 Tree-based regions grouper

Task

Modify the conventional tree-based grouper, introduced in section 3.3.2.1, in order to add the spatial condition defined in section 4.2 and use the new beamforing methods in order to estimate the SINR.

Description

This new grouper modifies the class `SINR Heuristic` and `Tree Based`

`Grouper` of `libWNS` library and adds a new method `validGroup`, which determines if one group fulfills the spatial condition defined in section 4.2.

5.2.7 Sequence diagram

5.2.7.1 Direct zeros towards inter-cell users coordination

Uplink

As chapter 4 describes, the *Direct zeros towards inter-cell users* coordination for UL has three tasks: information exchange, direct zeros towards the interferers and estimate the SINR.

Figure 5.2 shows the sequence diagram of the information exchange. The `ULMap Colletor` class calls the function `informationTransmission` after the scheduling. If the BS has the turn of transmission, it saves the coordination message in a global array of the `Network Coordinator` class. This message is built by using the information of the MAPs.

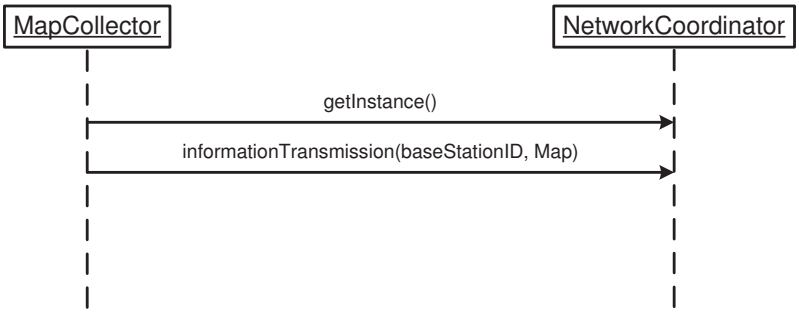

Figure 5.2: Simulation of information exchange

The sequence diagram 5.3 shows how one burst is scheduled with the *Zeros towards inter-cell users* coordination in UL. It is despicted how the scheduling information gathered by the `Network Coordinator` is provided to the BS and how it is further processed. The second and third task are performed by the strategy module: `RoundRobinUL` class, supported by the `Network Coordinator` and `Beamforming` classes. `RoundRobinUL` class calls the `getAllInterferings` method to obtain the Station Information of all possible interferers, that information is saved as `Interferings`. The `getCurrentInterferings` method detects the active interferers at `startTimeBurst` time and saved them and their Station Information as `currentInterferings`. The `timeOfFirstChange` returns the start time of the next set of interferers. With these three methods the end time of the new burst is calculated and the active interferers during the burst are known, then the calculation of the beam pattern and the estimation of the SINR for this burst are the next steps. `RoundRobinUL` calls `calculateCandIsWithInterCell` and `calculateAndSetBeam` methods in order to estimate the SINR and calculate the beam pattern, using the information of the coordiantion message. The start time for the next burst is the end time of the current burst rounded to the OFDMA symbol duration.

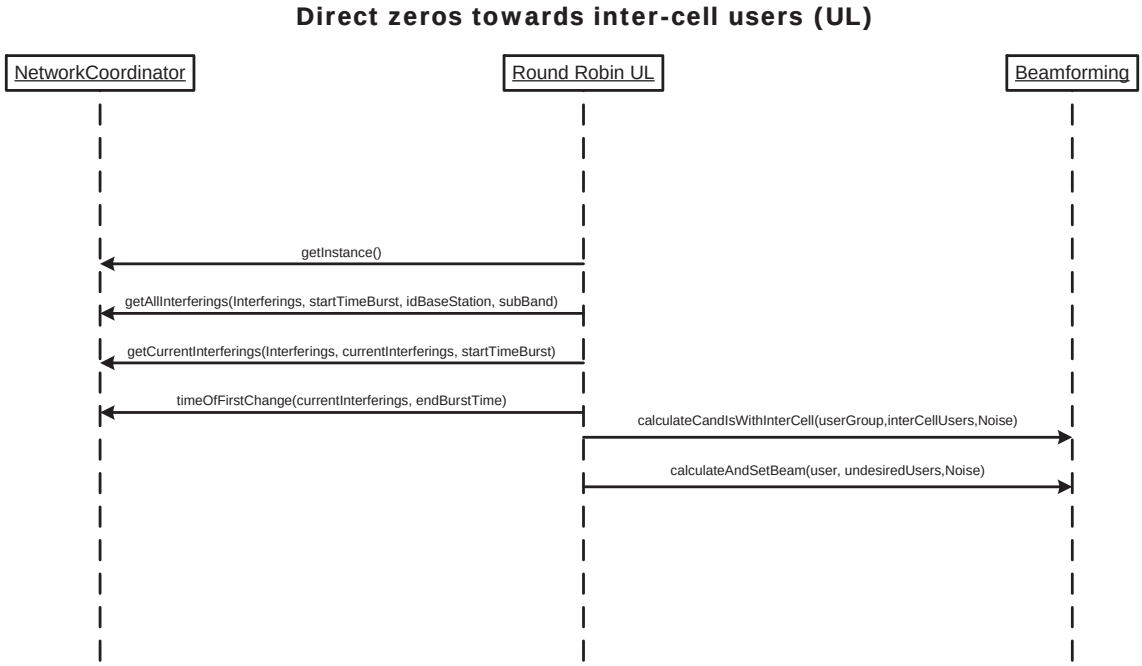

Figure 5.3: Scheduling of one burst (UL)

Downlink

As in UL, the *Direct zeros towards inter-cell users* coordination for DL has three tasks: information exchange, direct zeros towards the interfered users and estimate the SINR.

The simulation of the information exchange in DL is the same as in UL, refer to figure 5.2. The coordination message is build by using the information of the MAPs and the interferers' beam pattern.

Figure 5.4 shows the sequence diagram of how one burst is scheduled with the *Direct zeros towards inter-cell users* coordination in DL. The second and third task are performed by the strategy module: `RoundRobinDL` class, supported by the `Network Coordinator` and `Beamforming` classes. `RoundRobinDL` class calls the `getAllInterferings` method to obtain the Station Information of all possible interfering and interfered users, that information is saved as `Interferings`. The `getCurrentInterferings` method detects the active interfering and interfered stations at `startTimeBurst` time and saves them and their Station Information as `currentInterferings`. The `timeOfFirstChange` returns the start time of the next set of interfered or interfering SSs or the time of the first change in the interferers's pattern, the minimum of both. With these three methods the end time of the next burst is calculated, and the active interfering and interfered stations during the burst are known, thus the calculation of the beam pattern and the estimation of the SINR for this burst are the next steps. `RoundRobinDL` calls `calculateCandIsWithInterCell` and `calculateAndSetBeam` methods in order to estimate the SINR (without the inter-cell interference) and calculate the beam pattern. In order to add the inter-cell interference, using the information of the coordination message the `RoundRobinDL` calls the `setInterferingsPathLoss` and `getInterferingsAntennaGain` to obtain the interferers' pathloss and antenna gain, and calls `newSINRestimation` to add the inter-cell interference. The start time for the next burst is the end time of the current burst rounded to the OFDMA symbol duration.

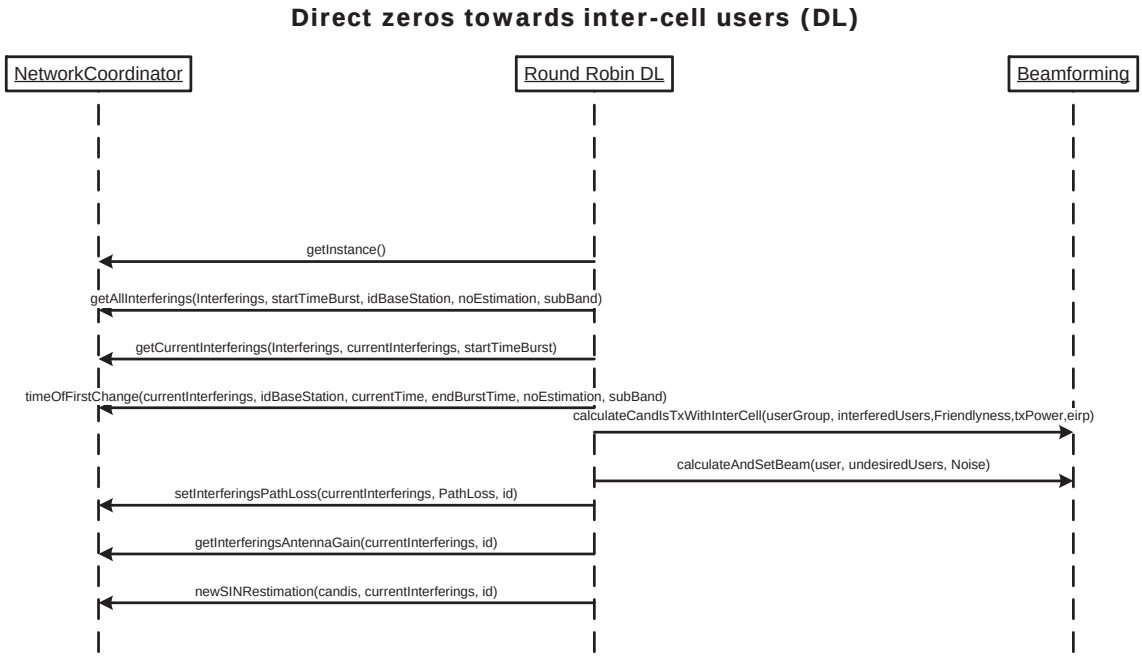

Figure 5.4: Scheduling of one burst (DL)

5.2.7.2 Spatial regions coordination

The *Spatial regions* coordination consists of three tasks: create the regions and the virtual SSUs, add the spatial condition inside the grouper and use the virtual SSUs in order to estimate the SINR.

Figure 5.5 shows the sequence diagram of how the modified grouper works in UL.

The `NetworkCoordinator` class builds the spatial regions and the virtual SSUs, with the methods `setRegions` and `setPositionOfVirtualStations`. These methods are called only one time, at the beginning of the simulation.

The addition of the spatial condition into the grouper and the use of the virtual SSUs in order to estimate the SINR are performed by the `Tree Based Grouper` and `SINRHeuristic` classes, with the support of the `Network Coordinator` class. Before to call the `treeAlgorithm` method, the grouper gets the position of the virtual SSUs using `getPositionOfVirtualStations` and gets the closest stations to them by means of `getClosestStation`. After that, the `treeAlgorithm` is called. When the new groups are built, `groupingUtility` method is called to calculate their throughput. Inside this method is called `validGroup` method which returns false if the group does not fulfill the spatial condition, and then this group is not used. In order to check the spatial condition inside the `validGroup` method, `getRegion` method of `Network Coordinator` class is called. It returns the subregion number of the group members, and if the value of one digit of the subregion numbers is repeated, the group is not valid. In the estimation of the SINR and the calculation of the beam pattern, the virtual SSUs are used as inter-cell interferings inside the `calculateCandIsWithInterCell` method and as undesired inside the `calculateAndSetBeam` method.

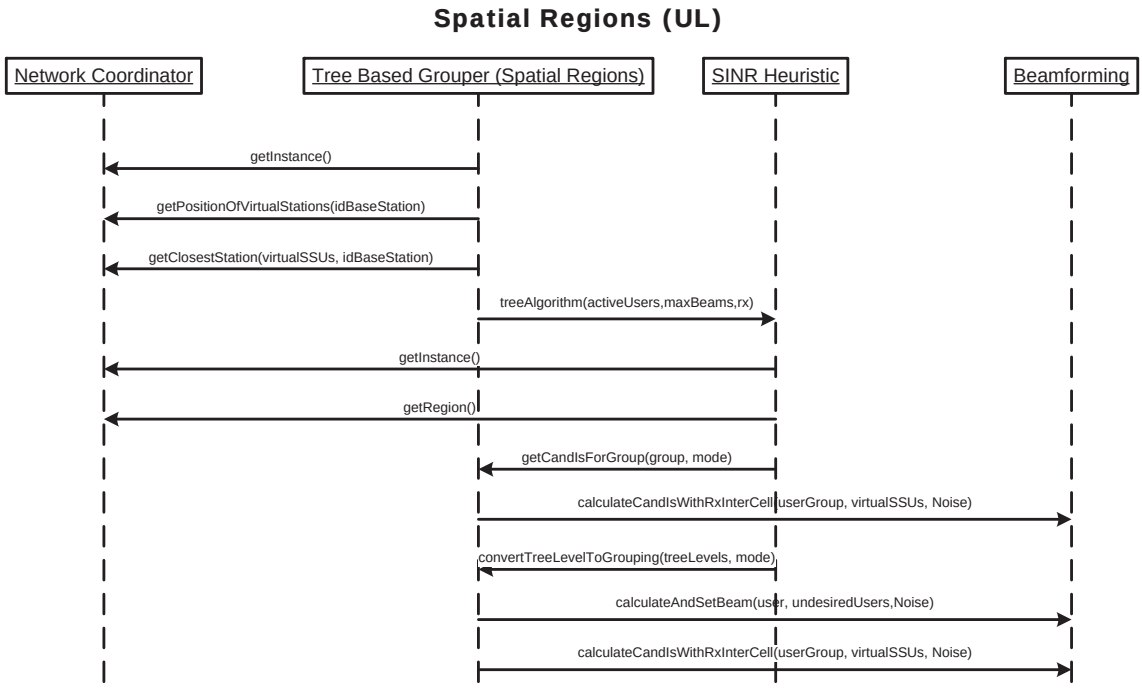

Figure 5.5: The tree-based SINR heuristic grouper with spatial regions concept

CHAPTER 6

Performance Evaluation

6.1 Scenarios and WiMAX simulation setup

6.1.1 Cellular single-hop scenario

The scenario consists of seven hexagonal cells with three sectors, each cell with a central BS and a variable number SSs, randomly situated in one sector of each cell. Measurements are only performed in openWNS for the central cell. Stations in the co-channel cells are not evaluated, but they generate interference to the central cell, with the same average traffic load as the stations of the central cell. The BSs of the seven cells work synchronosly in TDD: the start time of the DL and UL subframes are the same in every BS.
Figure 6.1 shows the multicell scenario. The black sector is the evaluated one. The red sectors have the same frequency band.

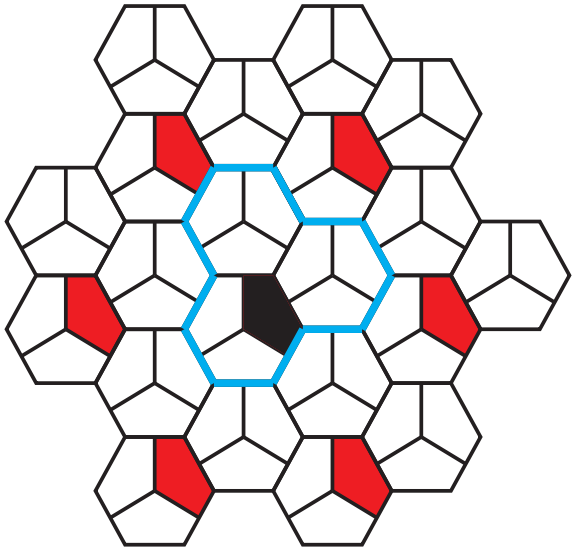

Figure 6.1: 3 cell cluster with 3 sectors

6.1.2 Performance metrics

MAC Throughput

The amount of user data of all MAC frames successfully arriving at the WiMAX MAC Service Access Point (SAP) during a fixed time window. Separate values are measured for packets traveling to/from every SS in UL and DL direction.

Delay

Measured at the destination station's MAC SAP for all packets that are successfully transmitted. Defined as the time elapsed between entering the sender's WiMAX protocol layer until leaving it at the receiver's MAC SAP. All delays experienced in buffers are counted. Under overload conditions the mean delay values are only in

partly meaningful, because the infinite delay of packets that are no transmitted is neither included in mean values nor counted.

Interference
Measured at the destination station's receiver (in dBm). All concurrent transmissions in co-channel cells (inter-cell interference) and all concurrent transmissions of the own cell (intra-cell interference) are accounted for. The interference level is averaged during packet reception. It also includes the thermal noise and the noise figure of the receiver.

Delta Interference
Difference between measured interference at the destination station's receiver and estimated interference at the BS of the cell.

Carrier
Signal strength during packet reception measured at the destination station's receiver (in dBm). Transmit as well as receive antenna gain is taken into account. The carrier signal is averaged during packet reception.

SINR
Calculated as the ratio between carrier and interference signal strength in dB.

MCS
Measured by the receiver as the MCS used for the packet.

Delta MCS
Measured by the receiver as the difference between the MCS number that would have been optimal (based on the measured SINR and on the threshold values [refer to Table 6.1]) and the MCS used for the packet. Positive values mean that the link adaptation was conservative. Negative values mean that the link adaptation was optimistic, and the MCS used cannot be afforded.

Buffer lost packets
Number of dropped outgoing packets in the buffer once it is full.

Cyclic Redundancy Check (CRC) loss ratio
Calculated as the ratio between the dropped packets at the CRC module and the total received packets in percentage.

6.1.3 Link adaptation and error schemeling

The link adaptation is performed in the WiMAC scheduling strategy. For each packet, the accordingly to the estimated SINR the MCS is choose. Table 6.1 despicts the SINR threshold of each MCS with a maximum BER of 10^{-6}. The estimated SINR determines the MCS with the next lower threshold. Figure 6.2 presents the Block Error Ratio (BLER) versus SNR, namely the information contained in the link level look-up table used in the openWNS to convert the SINR calculated into the Packet Error Rate (PER)[18].

6.1.4 WiMAX protocol settings

In the CBR and VBR traffic scenario the three concepts of coordination are studied and compared with the uncoordinated SDMA operation: *direct zeros towards inter-cell users coordination*, *direct zeros towards inter-cell users (one burst per group) coordination* and *spatial regions coordination*.

No.	Modulation	Code rate	Min. SINR $[dB]$	PHY data rate $[MBit/s]$
1	QPSK	1/2	5.0	14.93
2	QPSK	3/4	8.0	22.4
3	16 QAM	1/2	10.5	29.87
4	16 QAM	3/4	14.0	44.80
5	64 QAM	2/3	18.0	59.73
6	64 QAM	3/4	20.0	67.20

Table 6.1: Switching thresholds and PHY data rates for the modulation and coding schemes (PHY-schemes) used by the WiMAX simulations. [3]

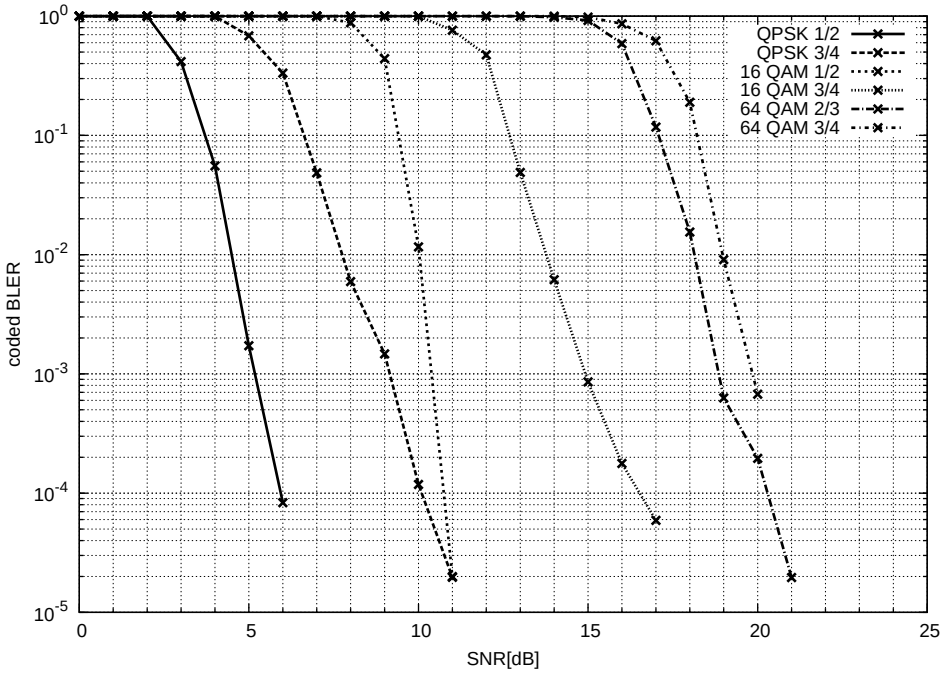

Figure 6.2: Coded BLER for AWGN channels

Parameter	Value
Frame/sec	25 frames/s
Group of Pictures (GOP)	N=12, M=3
Mean BW for compressed stream	0.55 Mbps
I frame size(Byte)	Negative Exponetial μ = 5700
P frame size(Byte)	Negative Exponetial μ = 3040
B frame size(Byte)	Negative Exponetial μ = 2280

Table 6.2: MPEG4 parameters

For the first concept the scheduler uses the strategy Segmented Round Robin, for the second one Round Robin and for the last concept Proportional Fair. In the first and the second coordination concept the spatial grouper uses the tree-based SINR heuristic. In the third coordination concept, it uses the tree-based regions SINR heuristic.

6.1.5 Simulation parameters

Each BS is equipped with a 12-element uniform linear antenna array used to serve one sector. SSs are equipped with omnidirectional antennas. For BSs, the transmit power is 44.23 dBm for a sector. For SSs, the transmit power is 23 dBm. The height of the BSs is 32 meters and the height of the SSs is 1.5 meters. A bandwidth of 20 MHz with a mid frequency of 2.5 GHz is used. Thermal noise (-174 dBm/MHz) is considered and a noise figure of 5 dB for BS or 7 dB for SS is added.
The "LOS C2" pathloss schemel based on [1] is used for the urban environment studied. Neither shadowing nor fast fading are considered.
The estimation of the station positions is perfect and the direction of the antenna beams is certain.
In order to eliminate the influence of particular SSs' positions, SSs are moving inside their sector. SSs follow a brownian motion with a speed of 30 km/h, handovers do not need to be considered.
The packet size is fixed, 190 Bytes. The SSs have a symmetric traffic load in DL and UL.
In the CBR traffic scenario the Inter Arrival Time (IAT) of packets is fixed, with the following value:

$$IAT[s] = \frac{\#(SS) \cdot PacketSize}{OfferedTraffic} \frac{Bit}{Bit/s} \tag{6.1}$$

In the VBR traffic scenario, the traffic used is the MPEG4 for high quality movie trace with a resolution for a small device [19]. Table 6.2 shows the MPEG4 parameters.
In order to emulate an OFDMA PHY layer, the subchannels are built in time domain. The OFDMA symbol duration and the number of subcarriers used for data transmission are reduced by the number of subchannels.
Legend notation:

- **No coordination**: uncoordinated SDMA operation
- **Coordination direct zeros**: direct zeros towards inter-cell users coordination
- **Coordination 1 burst per group**: direct zeros towards inter-cell users (one burst per group) coordination
- **Coordination regions**: spatial regions coordination

Table 6.3 shows the most important simulation parameters and their values.

Parameter	Value	Comment
Cluster Order	3	One tier of interfering cells
Cell radius	333 [m]	Based on [5]
Mobility	Brownian motion velocity = 30 km/h	Intra-cell mobility only
Number of sectors	3	Based on [5]
BS Height	32 [m]	Based on [5]
SS Height	1.5 [m]	Based on [5]
BS Noise Figure	5 dB	Based on [5]
SS Noise Figure	7 dB	Based on [5]
Mid frequency	2.5 GHz	Based on [5]
Pathloss	Urban macro-cell LOS	WINNER II LOS C2 [1]
Shadowing & Fast Fading	No	
Antenna array/elements	ULA / 12	Only at the BS
Max. beams	4	
Bandwidth	20 MHz	
BS Tx Power per sector	44.23 dBm [49dBm / 3 sectors]	Based on [5] (for Bandwidth (BW) 20MHz)
SS Tx Power	23 dBm	Based on [5]
Link adaptation	Adaptive	SINR threshold in Table 6.1
Traffic load UL/DL	Symmetric	
Packet size	190 Bytes	For data transmission
MAC Frame length	5 ms	Based on [5]
Number of subchannels	32	
Data carriers	48	
Subbands	1	All data carriers form one frequency channel
OFDMA symbol duration	3.214 μs	
ARQ	None	
Buffer size	500 packets	
Scheduling strategy: No coordination Coordination direct zeros Coord. 1 burst per group Coord. regions	 Proportional Fair Segmented Round Robin Round Robin Proportional Fair	
Spatial grouper: No coordination Coordination direct zeros Coord. 1 burst per group Coord. regions	 Tree-based SINR heuristic Tree-based SINR heuristic Tree-based SINR heuristic Tree-based regions SINR heuristic	

Table 6.3: Simulation parameters

6.2 Performance evaluation - Simulation results

6.2.1 CBR traffic scenario

6.2.1.1 10 SSs per sector

In this scenario *No coordination* and *Coordination direct zeros* approaches are compared.

Downlink

Figure 6.3 shows DL PDF MCS at 10 Mbps offered traffic which presents the MCS selection for the packets transmitted. The convetional SDMA operation can be highly enhanced by coordination, the number of packets with the highest MCS is increased by 20%. With coordination the BS directs zeros towards the interfered SSs, therefore the inter-cell interference is decreased and the SINR is increased.
Figure 6.4 shows the PDF of the Delta MCS in DL an offered traffic of 10 Mbps. With coordination more than 90% of the packets used the correct MCS. Compared to *No coordination* scheme the correct MCS selection is increased by 50%. Futhermore, without coordination about the 22% of packets are unsuccesful transmitted with a MCS which needs a higher SINR. In the *Coordination direct zeros* scheme this percentage is reduced to 1%. This result shows that the coordination enables better inter-cell interference estimation, the errors in the link adaptation are highly reduced by 2100%.

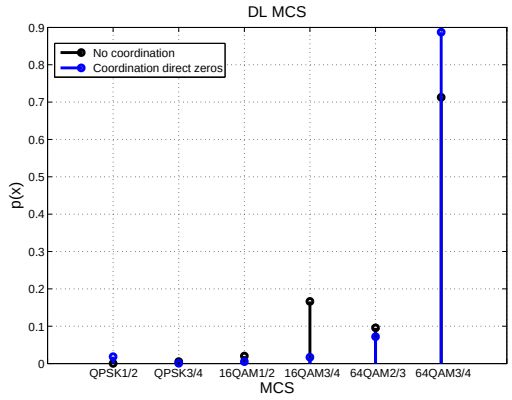

Figure 6.3: DL PDF MCS at 10Mbps offered traffic

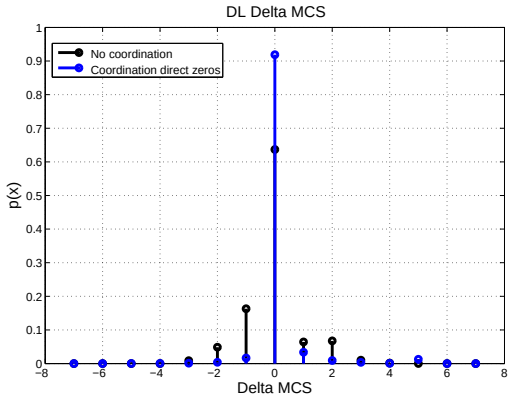

Figure 6.4: DL PDF Delta MCS at 10Mbps offered traffic

Figure 6.5 shows the Mean CRC loss ratio in DL. The lost packets ratio is significantly reduced by coordination due to better inter-cell interference estimation. The number of packets with a wrong MCS selection is decreased by coordination (refer to Figure 6.4), therefore the possibility of dropped packets within CRC module is also reduced.
Only with a low offered traffic the *Coordination direct zeros* scheme does not improve the *No coordination* scheme. This is because with that low traffic and with the packet size used, no all the users have packets to transmit in every frame, therefore the coordination information is not reliable.
Figure 6.7 depicts the mean DL MAC throughput. In the *Coordination direct zeros* scheme, the throughput increases linearly with the offered traffic up to 75 Mbps. In the *No coordination* scheme the throughput increases linearly with the offered traffic up to 10 Mbps. By mean of coordination the throughput capacity is significantly increased (650%). Due to the high CRC loss ratio in the *No coordination* scheme its throughput cannot increases

linearly with the increased offered traffic. The increase of the CRC loss ratio with 80 Mbps offered traffic has a significant impact in throughput. In the coordination scheme the packets use a higher MCS than the packets of the *No coordination* scheme (refer to Figure 6.3), therefore the *Coordination direct zeros* scheme can afford more traffic. The offered traffic does not account for the overhead, therefore the MAC throughput is higher than the offered traffic; 13.7% i.e. 208 bits overhead.
Figure 6.8 depicts the DL mean packet delay. The mean delay starts at a level of about 5ms and increases once the system saturates, around 75 Mbps offered traffic for both schemes. There is no retransmissions, therefore the packet loss effect is not take into account in the mean delay.
The number of lost packets of the buffer shown in Figure 6.6 confirms the aforementioned saturation points. The number of lost packets in coordination is lower than no coordination due to the higher throughput capacity of the *Coordination direct zeros* scheme.

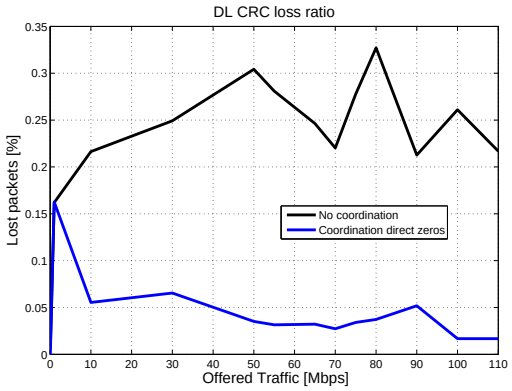

Figure 6.5: DL Mean CRC loss ratio

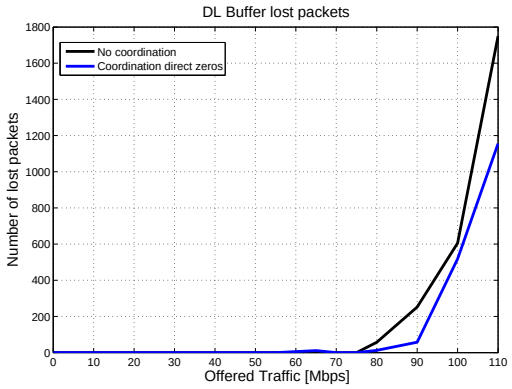

Figure 6.6: DL Buffer lost packets

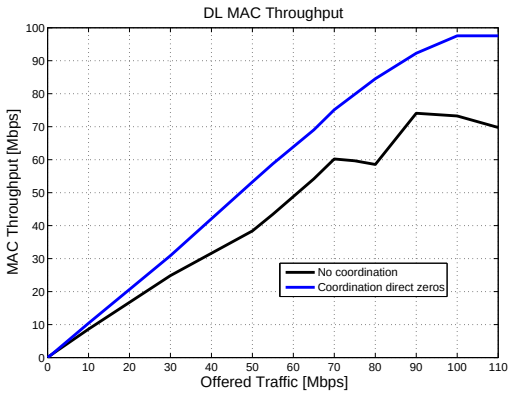

Figure 6.7: DL Mean MAC Throughput

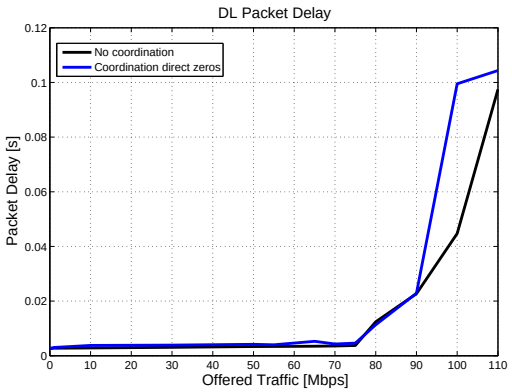

Figure 6.8: DL Mean Packet Delay

Uplink

In UL, the *Coordination direct zeros* scheme outperforms the *No coordination* in terms of link adaptation. Figures 6.9 and 6.10 show for an offered traffic of 10 Mbps the PDF of the MCS and the delta MCSs in UL. In the coordinated system, the number of packets which use the highest MCS is increased by 15%. In *No coordination* scheme the highest modulation is used by the 75% of the packets. The *Coordination direct zeros* scheme raises

this mean by 15%. Futhermore, the link adaptation is more reliable with coordination, more than 90% of the total packets have the correct MCS. Without coordination less than 70% of the packets have the correct MCS and almost 20% of the packets use a MCS that needs a higher SINR. The coordination improves the inter-cell estimation and mitigates it.

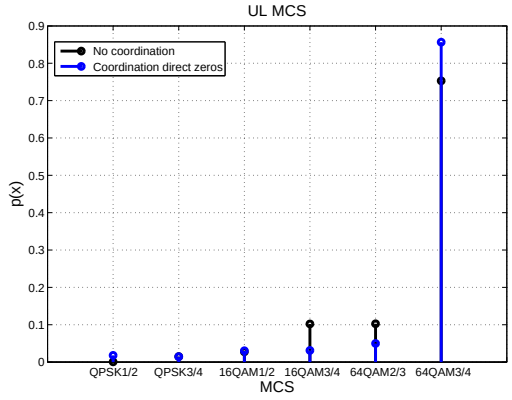

Figure 6.9: UL PDF MCS at 10Mbps offered traffic

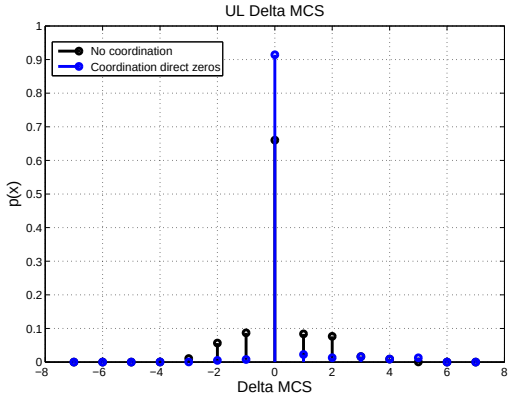

Figure 6.10: UL PDF Delta MCS at 10Mbps offered traffic

Figure 6.11 shows CRC loss ration in DL. This ratio confirms that the coordination improves the reliability of the system. In average, the double of packets are lost in the *No coordination* scheme. As mentioned above, with a low traffic due to the packet size, the *Coordination direct zeros* scheme has a bad performance.

In the Figure 6.13 the UL mean MAC throughput is presented. Without coordination, the throughput increases linearly with the increased offered traffic up to 10 Mbps. In the coordinated system, the throughput increases linearly up to 70 Mbps. The coordinated system increases the throughput capacity by 700%. Due to the high packet lost ratio in the CRC module, the throughtput of the *No coordination* scheme is importantly lower than the throughput of the *Coordination direct zeros* scheme. The increase of the CRC loss ratio with 80 Mbps offered traffic has a significant impact in throughput. Moreover, as Figure 6.9 shows, in the *Coordination direct zeros* scheme the packets use a higher MCS than the packets of the *No coordination* scheme, therefore the *Coordination direct zeros* scheme can carry more traffic.

Figure 6.14 presents the mean packet delay in UL. Without coordination the packet delay starts to increase around 1 Mbps offered traffic, and with coordination the packet delay starts to increase 70 Mbps offered traffic.

Figure 6.12 shows the mean number of lost packets in the buffers in UL. Without coordination, the losses start around 10 Mbps. The coordinated system starts to lose packets of the buffer around 70 Mbps offered traffic.

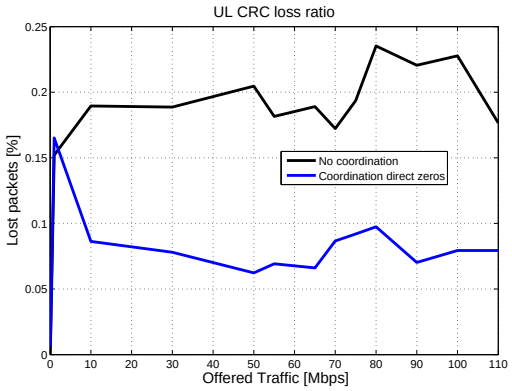

Figure 6.11: UL CRC loss ratio

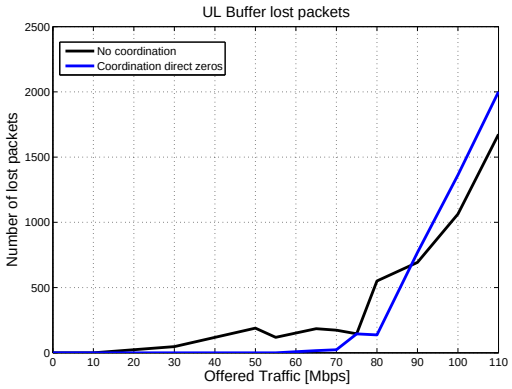

Figure 6.12: UL Buffer lost packets

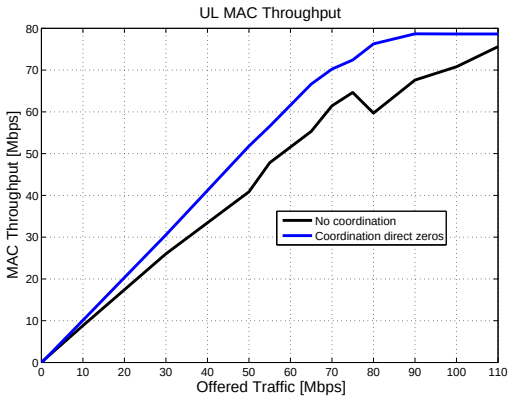

Figure 6.13: UL Mean MAC Throughput

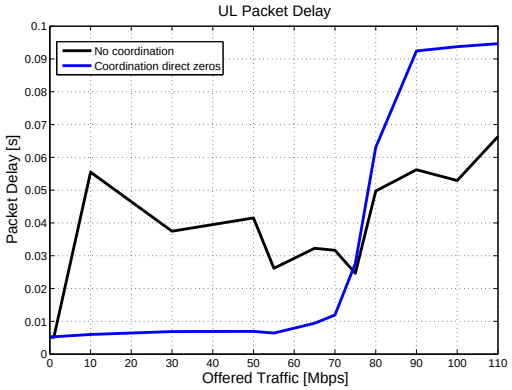

Figure 6.14: UL Mean Packet Delay

6.2.1.2 30 SSs per sector

When in the interfering/interfered cells the number of groups is different, within the scheduling of the *direct zeros towards inter-cell users coordination* scheme many burst are built for each group, therefore their duration decrease. Depending on the packet size and the MCS used the burst could not be filled with data.
In the following scenario this problem is studied. Additionally *Coordination 1 burst per group* and *Coordination regions* are studied.

Downlink

Figure 6.15 presents the PDF of the MCS in DL at an offered traffic of 10 Mbps. Without coordination, the mean MCS selected for transmitted packets is lower than in the coordinated systems. Less than 65% of the packets use the highest MCS. The best coordinated system in terms of MCS selection is the *Coordination direct zeros*, more than 80% of the packets use the highest MCS.
The PDF of the Delta MCS is shown in Figure 6.16. This figure confirms that by means of the *Coordination direct zeros* scheme the link adaptation becomes more reliable. With *Coordination 1 burst per group* scheme, Figure 6.16 shows that almost 30% of the packets could use better MCS. Because the *Coordination 1 burst per group* considers all the interferers for the whole burst, the inter-cell interference is pessimistic and for that reason

the MCS selection is also pessimistic. *Coordination regions* has a significant percentage of packets with a MCS which cannot be afforded (17%). This is because this coordination method mitigates the interference but it is not designed to improve the inter-cell interference predictability. Figure 6.16 shows that with this method the mean MCS selected for the packets transmitted is higher than the used in the *No coordination* scheme.

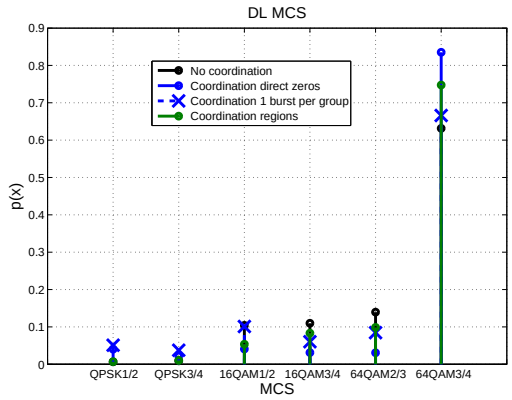

Figure 6.15: DL PDF MCS at 10Mbps offered traffic

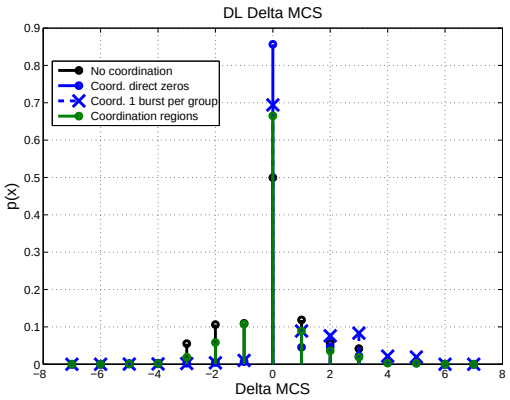

Figure 6.16: DL PDF Delta MCS at 10Mbps offered traffic

In Figure 6.17 is shown the CRC loss ratio in DL. This ratio confirms better SINR estimation performance of the *Coordination direct zeros* and *Coordination 1 burst per group* schemes. The *Coordination regions* improves the *No coordination*, however this improvement is because the inter-cell interference reduction.

Figure 6.19 shows the mean MAC throughput in DL. The three coordinated schemes outperforms the uncoordinated. Futhermore, *Coordination 1 burst per group* enhances *Coordination direct zeros* when the problem of many small burst happends. Compared to *No coordination* scheme, *Coordination direct zeros* and *Coordination 1 burst per group* schemes the throughput capacity is increased by 680% due to these schemes reduce CRC loss ratio and the mean MCS is higher.

Figure 6.20 shows the mean packet delay for the four schemes in DL. In the *Coordination 1 burst per group* scheme, the packet delay starts to increase slightly around 15 Mbps offered traffic. Around 50 Mbps offered traffic, the packet delay starts to increase highly. The packet delay of *Coordination direct zeros* and *Coordination regions* schemes increases around 50 Mbps offered traffic. The delay of *No coordination* scheme increases around 55 Mbps offered traffic.

The mean number of lost packets of the buffers is shown in Figure 6.18. *Coordination direct zeros* and *Coordination regions* start to lose packets around 50 Mbps offered traffic. *No coordination* and *Coordination 1 burst per group* schemes start to lose packets around 60 Mbps offered traffic.

Based on Figures 6.20 and 6.18, in *Coordination regions* and *Coordination 1 burst per region* the system saturates around 50 Mbps offered traffic. In *Coordination direct zeros* and *No coordination*, saturates around 55 Mbps offered traffic.

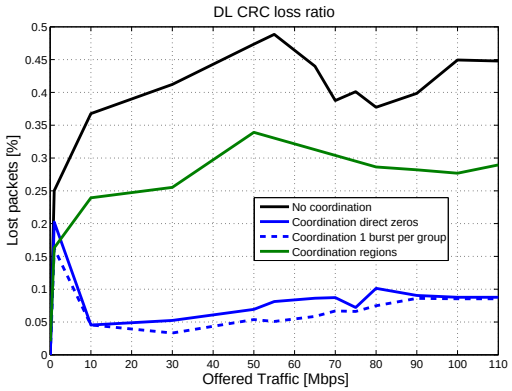

Figure 6.17: DL CRC loss ratio

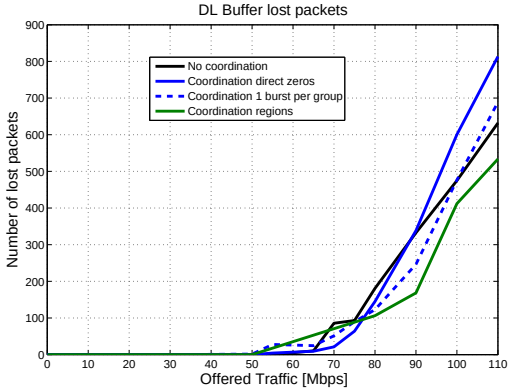

Figure 6.18: DL Buffer lost packets

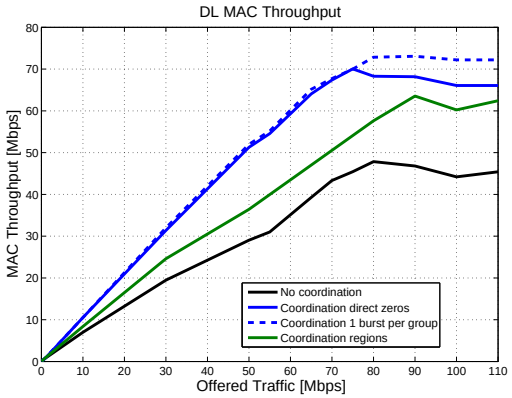

Figure 6.19: DL Mean MAC Throughput

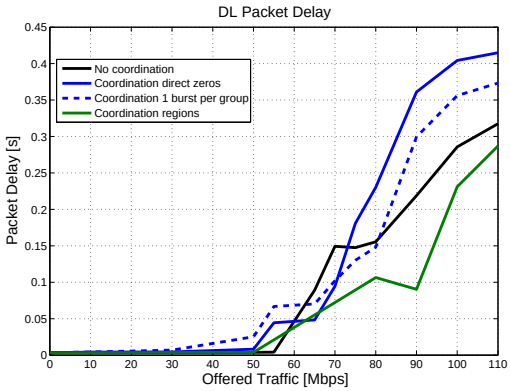

Figure 6.20: DL Mean Packet Delay

Uplink

The Figures 6.21 and 6.22 show the better behavior of the coordinated systems in relation to link adapatation. By using the new beamforming strategy the coordination schemes improve the SINR, and also its estimation is highly improved by mean of the different coordination strategies.

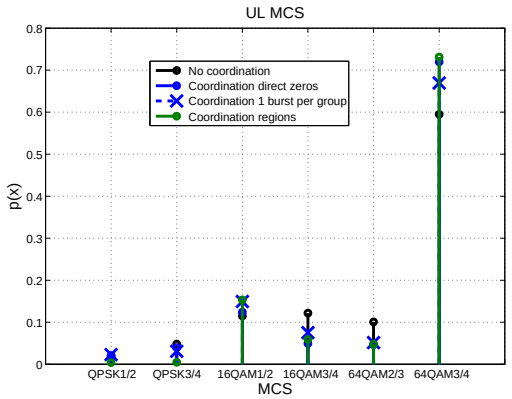

Figure 6.21: UL PDF MCS at 10Mbps offered traffic

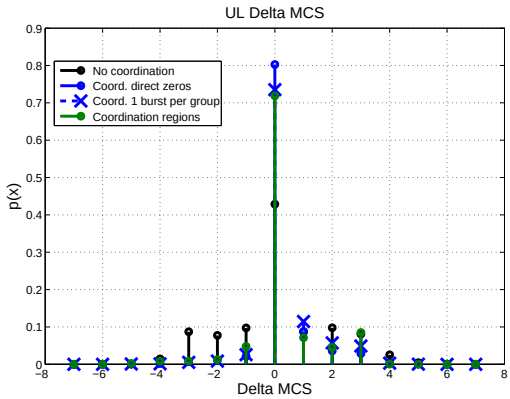

Figure 6.22: UL PDF Delta MCS at 10Mbps offered traffic

In Figure 6.23 is shown the UL CRC loss ratio. It confirms better behavior in terms of reliability of the coordination schemes. The percentage of lost packets is hugely decreased by the coordination schemes.
Figure 6.25 presents the UL mean MAC throughput. *Coordination regions* and *Coordination 1 burst per region* are the best schemes in throughput capacity. Due to the high CRC loss ratio the uncoordinated system is hugely enhanced by the aforementioned schemes. *Coordination direct zeros* scheme gets worse due to the unused time. The number of burst per group increases and their duration decreases, therefore the scheduling cannot fill all the burst with data. In *Coordination direct zeros* scheme, the CRC loss ratio variatons impact significatly the mean throughput.
Figure 6.26 shows the UL mean packet delay. In *Coordination regions* scheme, the packet delay increases around 1 Mbps offered traffic. *Coordination direct zeros* and *No coordination* schemes shift this point up to 10 Mbps offered traffic. In *Coordination 1 burst per group* scheme, the delay increases around 30 Mbps offered traffic. In *Coordination direct zeros* scheme, the throughput variatons impact significatly the mean throughput.
Figure 6.24 presents the number of lost packets of the buffer. *Coordination direct zeros* scheme starts to lose packets around 10 Mbps offered traffic. The other schemes shift this point up to 30 Mbps.
Based on Figures 6.26 and 6.24 *Coordination direct zeros* scheme saturates around 10 Mbps offered traffic. *Coordination regions*, *Coordination 1 burst per region* and *No coordination* schemes shift the saturation point up to 30 Mbps offered traffic.

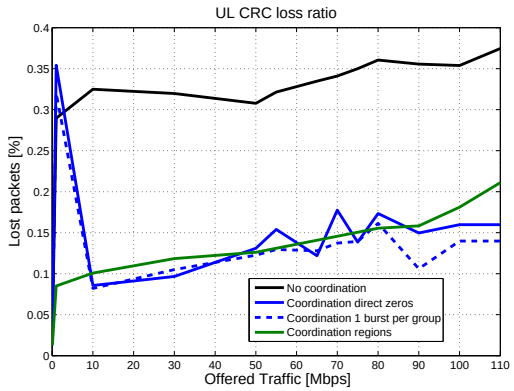

Figure 6.23: UL CRC loss ratio

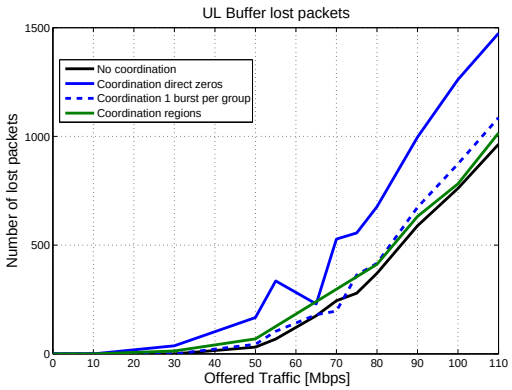

Figure 6.24: UL Buffer lost packets

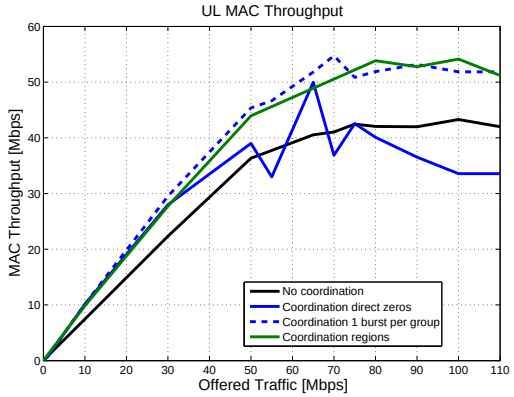

Figure 6.25: UL Mean MAC Throughput

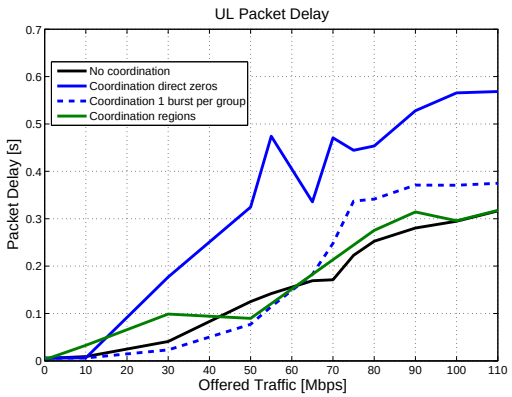

Figure 6.26: UL Mean Packet Delay

6.2.2 VBR traffic scenario

Consideration

In the following studies a MPEG4 traffic model for high quality movie trace with a resolution for a small device[19] is assumed with a mean data rate of 0.55 Mbps.
Due to the simulation limitation, the number of SSs per sector and the simulation time were not large enough in order to find the saturation point of all the schemes.
In order to increase the total offered traffic, the number of SSs per sector is increased.
The MPEG4 frames are segmented into small packets of 190 Bytes which are then distributed during the MPEG4 frames.

Downlink

Figure 6.27 shows the MCS at 10 Mbps offered traffic in DL. *Coordination direct zeros* and *Coordination regions* schemes enhanced the MCS selection of *No coordination* scheme, by using the higher MCS due to increased SINR [refer to Figures B.11 and B.12].
The reliability of the link adaptation is shown in Figure 6.28, DL delta MCS. Estimation errors for the MCS are reduced by all types of coordination. However *Coordination regions* has a significant percentatge of packets with a MCS which cannot be afford. This is because this coordination method mitigates the interference but it is not designed to improve the inter-cell interference predictability.
Because the *Coordination 1 burst per group* considers all the interferers for the whole burst, the inter-cell interference is pessimistic and for that reason the MCS selection is also pessimistic, the Figure 6.28 shows that almost 35% of the packets could use better MCS.

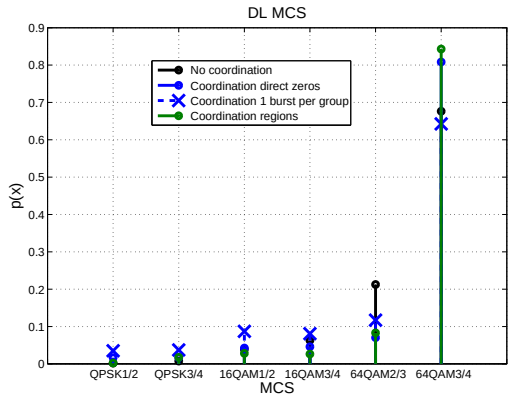

Figure 6.27: DL PDF MCS at 10Mbps offered traffic

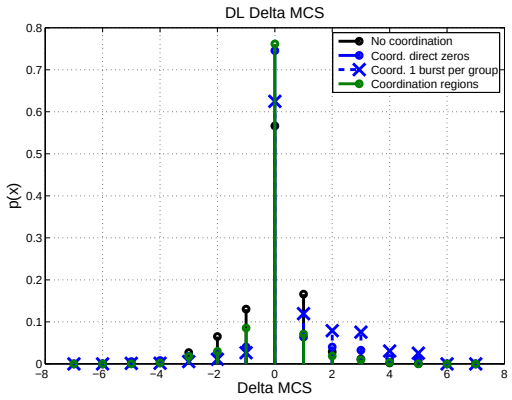

Figure 6.28: DL PDF Delta MCS at 10Mbps offered traffic

The CRC loss ratio in DL shown in Figure 6.29 confirms that the coordinated schemes are more reliable. The percentage of CRC lost packets in *No coordination* scheme is a lot higher than in *Coordination direct zeros* and *Coordination 1 burst per group* schemes. Compared to *Coordination direct zeros* scheme, in *Coordination 1 burst per group* scheme the MCS selection is pessimistic, for that reason the CRC loss ratio is lower.
Figure 6.31 depicts the mean MAC throughput in DL. *Coordination direct zeros* and *Coordination 1 burst per group* schemes improve the saturation throughput from 5 Mbps in the uncoordianted case up to around 25 Mbps.
After this point, some SS cannot be served. This is because the offered traffic is increased by increasing the number of SSs. In the Round Robin algorithm the length of the bursts

depends on the number of groups, therefore if the number of groups increases, the length of the bursts decreases, and higher MCSs are needed in order to be able to fill the bursts with data. Apparently when a SS cannot be served, its traffic is not generate within the BS, because outgoing packets are not dropped, as show in Figure 6.30.
Figure 6.32 shows the DL mean packet delay and Figure 6.30 shows the DL number lost packets in the buffer. Because the traffic generated by the unserved SSs is neglected, the number of lost packets of *Coordination direct zeros* and *Coordination 1 burst per group* schemes is 0. Therefore, these two schemes are in saturation with an offered traffic higher than 25 Mbps, because some SSs cannot transmit their packets. However the other SSs are able to transmit all their packets.

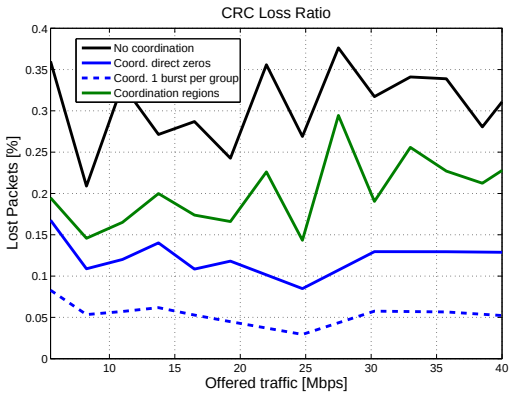

Figure 6.29: DL CRC loss ratio

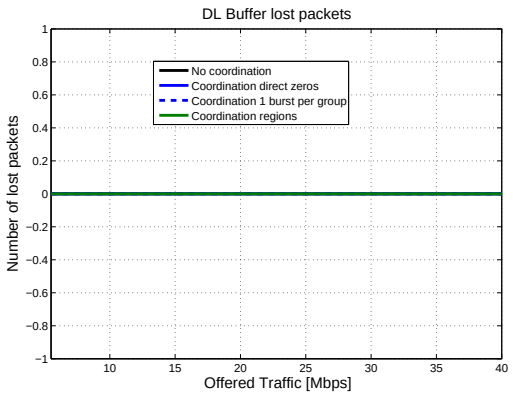

Figure 6.30: DL Buffer lost packets

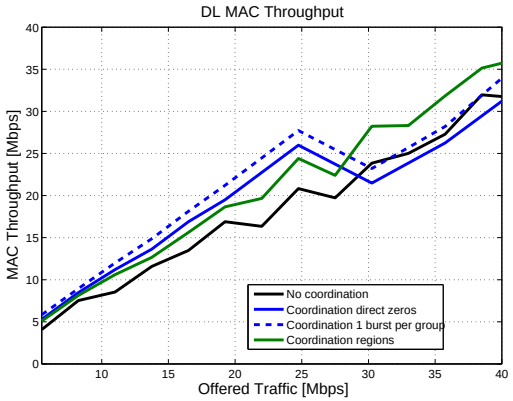

Figure 6.31: DL Mean MAC Throughput

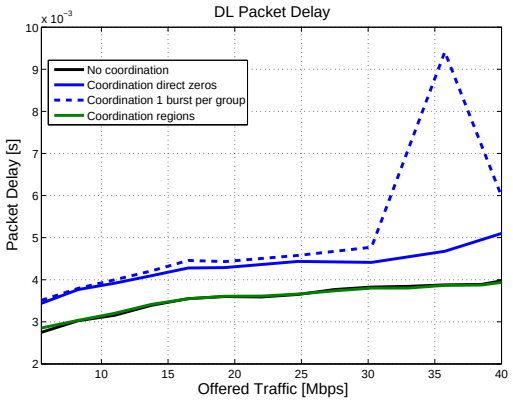

Figure 6.32: DL Mean Packet Delay

Uplink

Figure 6.33 shows the selected MCS at 10 Mbps offered traffic in UL. *Coordination direct zeros* and *Coordination regions* schemes enhanced the MCS selection of *No coordination* scheme due to the increase of SINR [refer to Figure B.21 and B.22].
The PDF of the delta MCS in UL is shown in Figure 6.34. The three coordination schemes outperforms the uncoordinated case, less packets are transmited with a wrong MCS. In the *No coordination* scheme more than 20% of the packets use a MCS which cannot be afforded. With coordination, the number of packets that use a wrong MCS is reduced to 10% in the worst case.

Because the *Coordination 1 burst per group* considers all the interferers for the whole burst, the inter-cell interference is pessimistic and for that reason the MCS selection is also pessimistic, the Figure 6.34 shows that almost 30% of the packets could use better MCS.

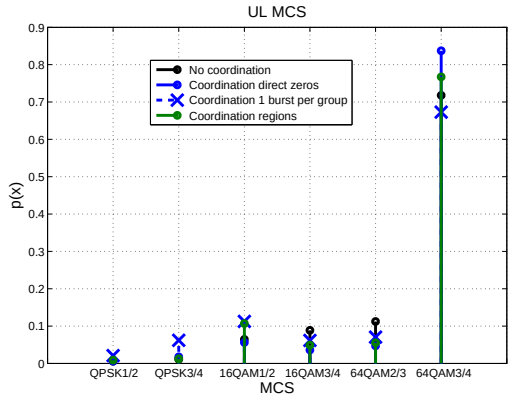

Figure 6.33: UL PDF MCS at 10Mbps offered traffic

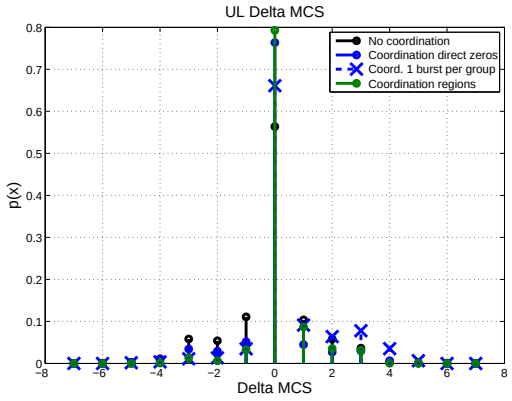

Figure 6.34: UL PDF Delta MCS at 10Mbps offered traffic

Figure 6.35 presents the CRC loss ratio in UL. The coordination schemes outperform the *No coordination*, specially *Coordination 1 burst per region*. Compared to the *No coordination*, *Coordination 1 burst per region* reduces the percentage of lost packets by 250%.
Figure 6.36 shows the mean MAC throughput in UL. *Coordination direct zeros* and *Coordination 1 burst per group* schemes outperform the saturation throughput from less than 10 Mbps with no coordination up to 25 Mbps. With more offered traffic, *Coordination regions* scheme has the best performance. As mentioned above, *Coordination direct zeros* and *Coordination 1 burst per group* schemes saturate due to the dependency between the number of groups and the burst length when a Round Robin scheduling strategy is employed.

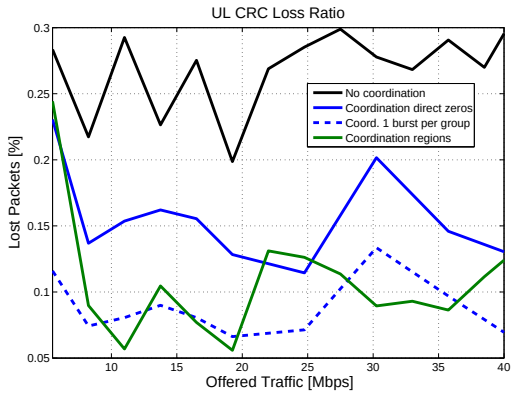

Figure 6.35: UL CRC loss ratio

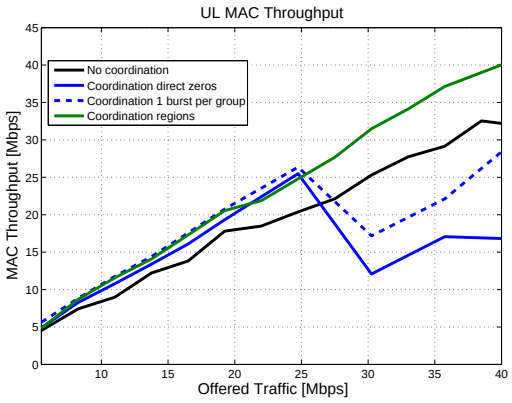

Figure 6.36: UL Mean MAC Throughput

Figure 6.37 shows the mean packet delay. In *Coordination direct zeros* and *Coordination 1 burst per group* schemes the mean packet delay start to increase around the 25 Mbps, once the system saturates. The mean packet delay of *No coordination* and *Coordination regions* schemes remains under 100ms (20 MAC frames). The mean delay value for this two schemes is higher than the other schemes due to the level of interference.
The number of buffer packet lost shown in Figure 6.38 confirms the saturation point of *Coordination direct zeros* and *Coordination 1 burst per group* schemes at 25 Mbps. In

Coordination regions scheme, the system starts to lose packets around 15 Mbps offered traffic. This is because some SSs cannot be served.

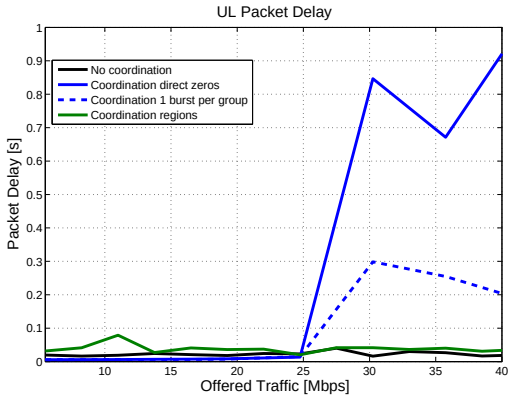

Figure 6.37: UL Mean Packet Delay

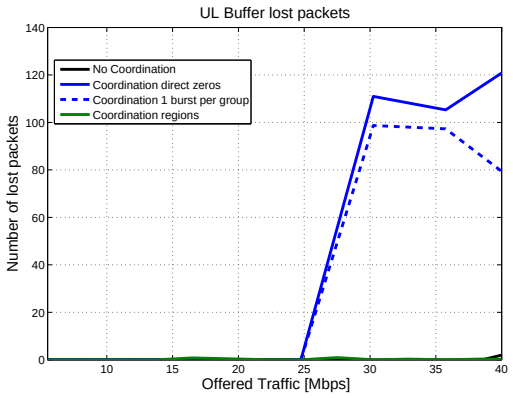

Figure 6.38: UL Buffer lost packets

6.2.3 Conclusion

In a CBR scenario, the use of coordination highly enhances the inter-cell interference estimation (except the *Coordination regions* scheme in DL) and its mitigation. The coordination schemes improve the link adaptation. With coordination the packets use higher MCS than without. Furthermore the link adaptation becomes more reliable, the number of the packets with the correct MCS increases and the CRC loss ratio decreases. Based on these improvements, the MAC throughput is highly improved. The best coordination scheme for CBR is the *Coordination direct zeros* scheme, however is limited by the amount of burst per group. In this scenario, *Coordination 1 burst per group* is the best scheme. In UL, the performance of *Coordination regions* scheme is equal to *Coordination 1 burst per group*.
In a VBR scenario, the use of coordination improves the inter-cell interference estimation (except the *Coordination regions* scheme in DL) and its mitigation. In general, by means of coordination schemes the link adaptation becomes more reliable: the number of the packets with the correct MCS increases and the CRC loss ratio decreases. Furthermore, with *Coordination direct zeros* and *Coordination regions* schemes the MCS used for the packet transmission is enhanced with respect to the *No coordination* scheme. Based on these improvements, the MAC throughput is enhanced by *Coordination regions* for every offered traffic. The MAC throughput is enhanced by *Coordination direct zeros* and *Coordination 1 burst per group* scheme from lower than 10 Mbps up to 25 Mbps. However with smaller packet size these two schemes could improve their saturation throughput.
Coordination direct zeros approach improves the system, but the complexity in terms of scheduling and beamforming is increased due to raised number of burst per group and amount of new zeros in the beam pattern. Furthermore, the exchange of information adds complexity to the network, and additional signalling overhead is generate.
With *Coordination 1 burst per group*, the complexity of the scheduling is decreased compared to *Coordination direct zeros* by reducing number of burst, but the beamforming complexity is increased, the BSs have to direct zeros towards more stations.
With *Coordination regions* only the complexity of the SDMA grouper and the beamforming is slightly increased.

CHAPTER 7

Conclusions And Outlook

This chapter summarizes the contributions of this thesis and gives an outlook for future research opportunities.

7.1 Summary

During this thesis three coordination schemes have been developed in order to increase the predictability of the inter-cell interference and to mitigate its strengh.
These coordination schemes have been implemented into the openWNS. Besides the coordination schemes, other modifications (such as sectorisation or mobility within a sector) have been implemented into the simulator in order to fullfil the IEEE 802.16m evaluation methodology.
Two traffic types (CBR and VBR) have been considered in the implemented simulator in order to evaluate the coordination schemes.
From results it can be derived that an approach which combine the different coordination schemes would further improve a SDMA enhanced system. In general, using coordination schemes the link adaptation becomes more efficient and reliable (packets use higher MCS and the MCS prediction is more precise), and the throughput capacity is enhanced.

7.2 Theses

Coordination across BSs:

- Mitigates inter-cell interference and increases its predictability.
- Improves system capacity and spectral efficiency.
- Increases system complexity and causes coordination overhead.

7.3 Outlook, future research opportunities

Based on the different coordination schemes presented in this thesis there are open enhancements for further research:
Spatial regions coordination:

- New spatial grouping for DL in order to improve the inter-cell estimation.

Direct zeros towards inter-cell users coordination and **direct zeros towards inter-cell users (one burst per group) coordination**:
The simulations have proved that the Round Robin and Segmented Round Robin have limited performance with a high number of SSs per sector due to the burst duration. In order to avoid this problem three solutions are proposed:

- Extend the Round Robin to many frames.
- Smaller packet size.
- Longer frame length.

For all coordination schemes:

- Consider other VBR traffic models (e.g. Gaming, VoIP, traffic mixes).
- Apply wrap around in order to check the impact of the second interfering ring.
- Study uncertainty in the direction of the antenna beams.
- Designing concepts considering relay stations.

APPENDIX A

Creation of spatial regions and virtual Spatial Super Users

Due to the shape of the sector is necessary to define a different strategy to calculate the area of the region for three situations:

1. $\beta > \alpha_a$.
2. $\beta = \alpha_a$.
3. $\beta < \alpha_a$.

For the first strategy, the parameters to calculate the area of the region are defined in the Figure A.1.

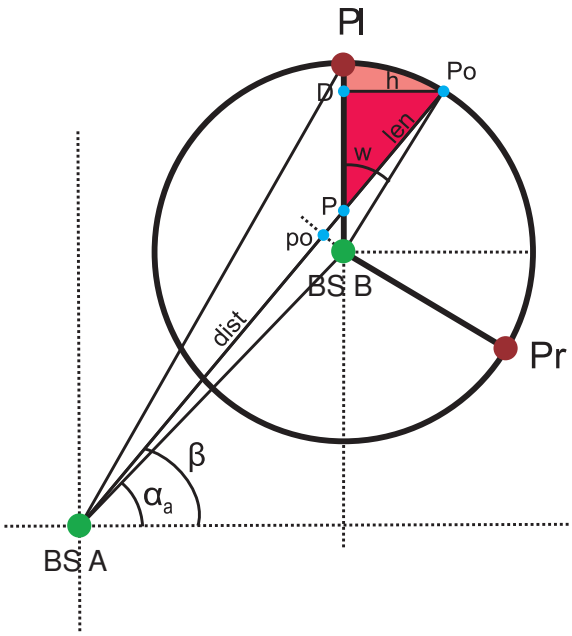

Figure A.1: Scenario for the first strategy

Where:

- α_a angle between the interfering and interfered BS.
- β angle of the imaginary line.
- $dist$ distance between the two base stations.
- $P = \sin(\pi/2 - a) \cdot \sin(a - \alpha_a) \cdot dist$.
- $Po = \sin(a - \alpha_a) \cdot dist + \sqrt[2]{(radius)^2 - (\sin(\alpha_a - a) \cdot dist)^2}$.
- w angular difference between the point omega and the point Po.
- $h = \sin(w) \cdot radius$.
- $D = \cos(w) \cdot radius$.
- $len = \sqrt[2]{(D - P)^2 + h^2}$.
- $po(r_o, \varphi_o)$ is the point created by the imaginary line and the line which crosses the interfering BS and is perpendicular to the imaginary line: $po = (interferedBS(x) + \cos(a) \cdot \cos(a - \alpha_a) \cdot dist, interferedBS(y) + \sin(a) \cdot \cos(a - \alpha_a) \cdot dist)$

- $r_o = \sqrt[2]{((po(y) - interferingBS(y))^2/(po(x) - interferingBS(x))^2)}$.
- $\varphi_o = \arctan((po(y) - interferingBS(y))/(po(x) - interferingBS(x)))$.
- $r(\theta)$ is the imaginary line expressed in polar coordinate system: $r(\theta) = r_o \sec(\theta - \varphi_o)$. The pole of the polar coordinate system is at the interfering BS.

$$Area = \int_{\pi/2-w}^{\pi/2} \int_{r(\theta)}^{radius} r\, drd\theta = (radius^2 \cdot w)/2 + (r_o^2 \cdot (\tan(pi/2 - \varphi_o) - \tan(pi/2 - w - \varphi_o)))/2 \tag{A.1}$$

For the second strategy, the parameters to calculate the area of the region are defined in the Figure A.2:

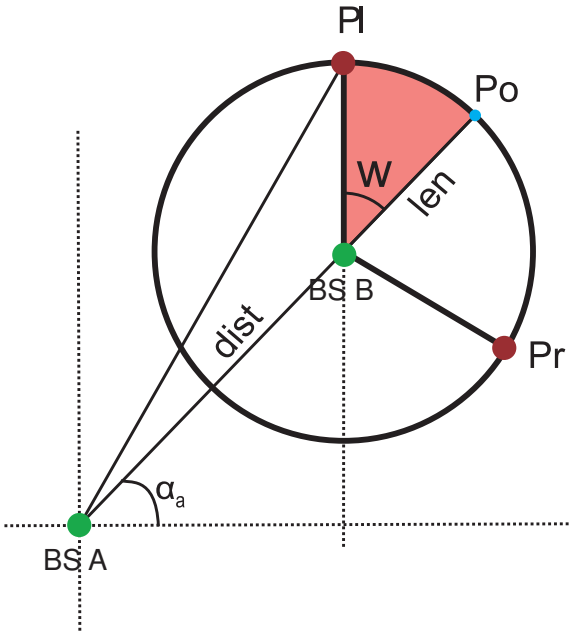

Figure A.2: Scenario for the second strategy

Where:

- w angular difference between the point alpha and the imaginary line.
- β angle of the imaginary line.
- $len = radius$.

$$Area = \int_{\pi/2-w}^{\pi/2} \int_{0}^{radius} r\, drd\theta = (radius^2 \cdot w)/2 \tag{A.2}$$

For the third strategy, the parameters to calculate the area of the region are defined in the Figure A.3:

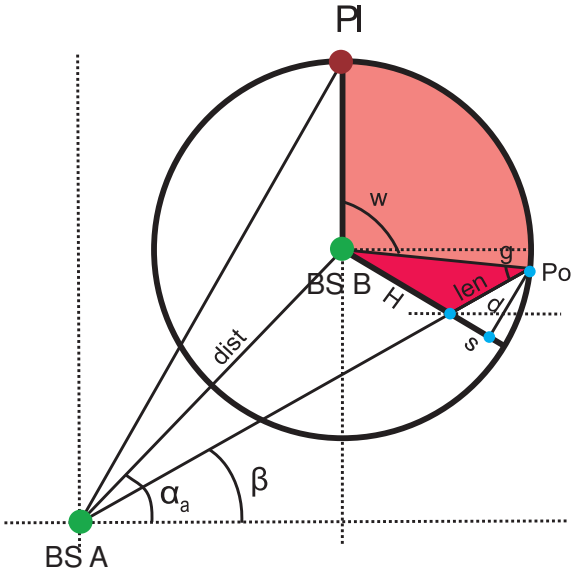

Figure A.3: Scenario for the third strategy

Where:

- α_a angle between the interfering and interfered BS.
- β angle of the imaginary line.
- *dist* distance between the two base stations.
- $Po = \cos(\alpha_a - a) \cdot dist + \sqrt[2]{(radius)^2 - (\sin(\alpha_a - a) \cdot dist)^2}$.
- w angular difference between the point omega and the point Po.
- $g = a + w - \pi/2$.
- $H = (radius \cdot \sin(g))/\sin(\pi - g - (2\pi/3 - w))$.
- $d = |\sin(2\pi/3 - w) \cdot radius|$.
- $s = |\cos(2\pi/3 - w) \cdot radius|$.
- $len = \sqrt[2]{(s - H)^2 + d^2}$

$$Area = \int_{\pi/2-w}^{\pi/2} \int_{0}^{radius} r\, dr d\theta + (H \cdot d)/2 = (radius^2 \cdot w)/2 + (H \cdot d)/2 \tag{A.3}$$

The SSUs are situated at the weight point of the regions, from the point of view of the interfered BS. The weight point is defined by two parameters: angle and distance. The angle of the weight point (β_{SSU})is calculated as the angle which divides the region in two regions with the same area. In order to calculate the distance, in each iteration the algorithm saved the width of the sector (paramater *len* in the three aforementioned strategies). Thus, the distance between the weight point and the interfered BS is the distance between the interfered BS and the *Po* point minus the half of the average of *len* (*hAveLen*). Figure A.4:

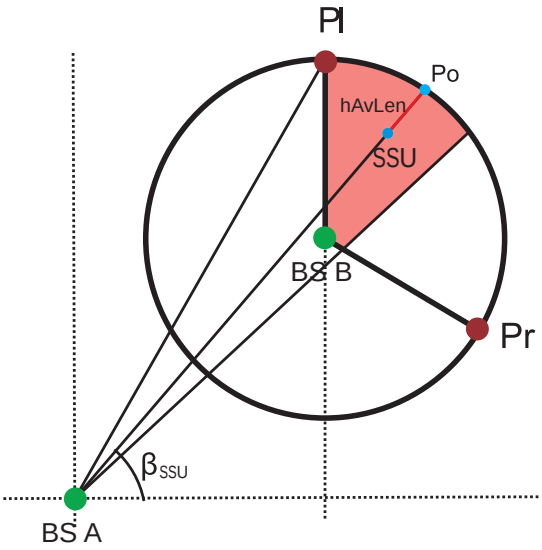

Figure A.4: Position of virtual SSU

APPENDIX B

Additional results

B.1 CBR scenario

B.1.1 10 SSs per sector

B.1.1.1 Downlink

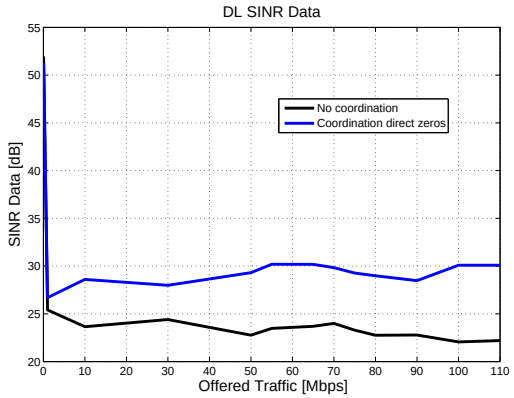

Figure B.1: DL Mean SINR Data

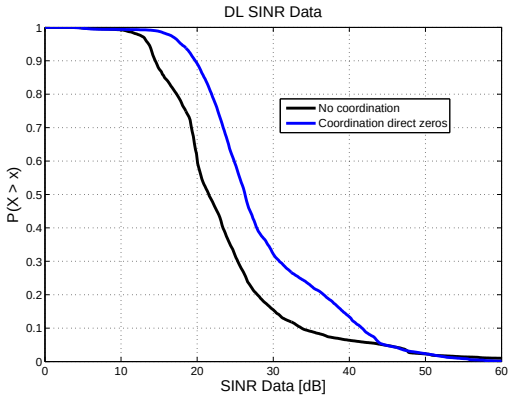

Figure B.2: DL CCDF SINR Data at 10Mbps offered traffic

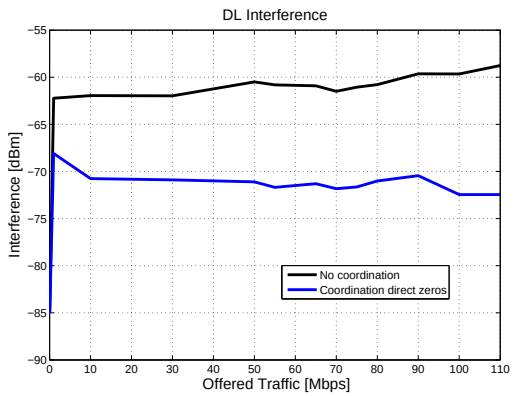

Figure B.3: DL Mean Interference

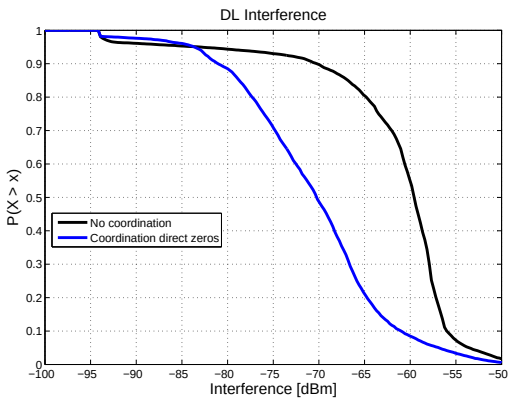

Figure B.4: DL CCDF Interference at 10Mbps offered traffic

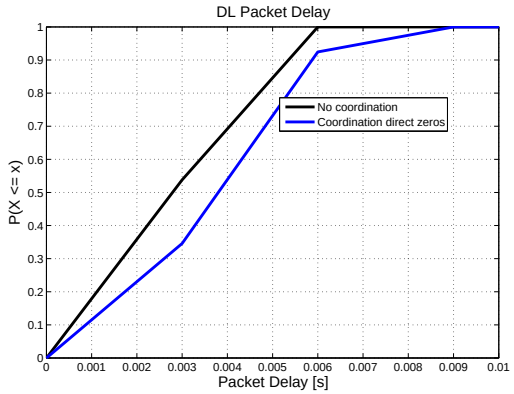

Figure B.5: DL CDF Packet Delay at 10Mbps offered traffic

B.1.1.2 Uplink

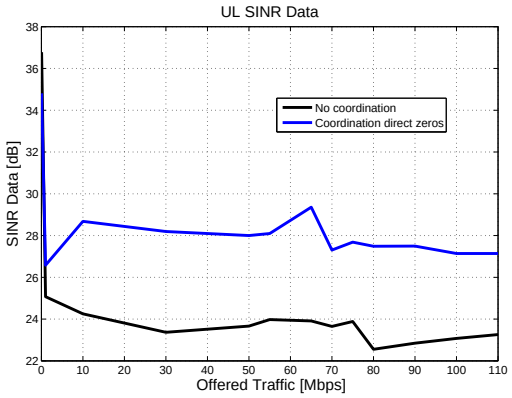

Figure B.6: UL Mean SINR Data

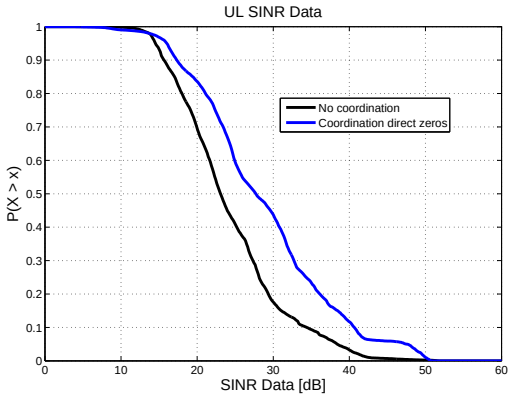

Figure B.7: UL CCDF SINR Data at 10Mbps offered traffic

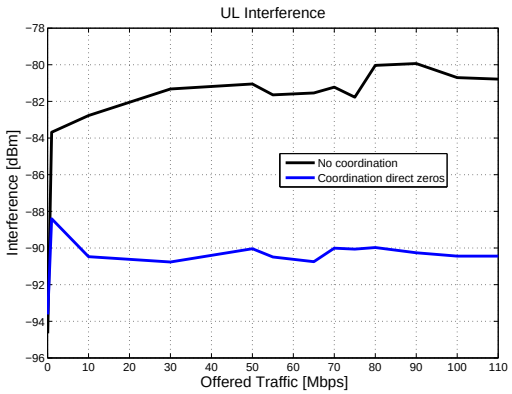

Figure B.8: UL Mean Interference

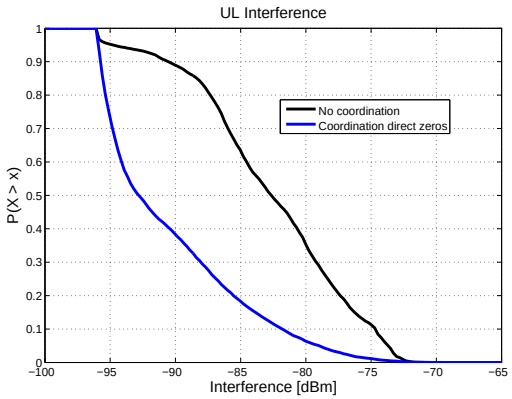

Figure B.9: UL CCDF Interference at 10Mbps offered traffic

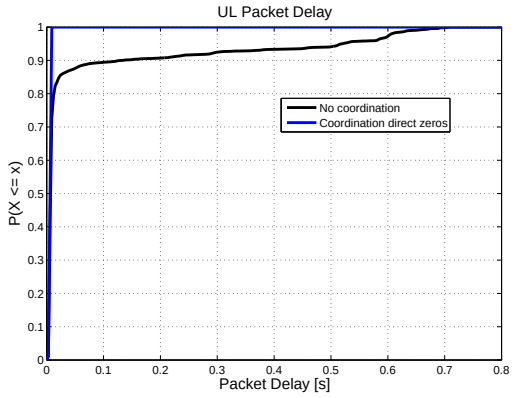

Figure B.10: UL CDF Packet Delay at 10Mbps offered traffic

B.1.2 30 SSs per sector

B.1.2.1 Downlink

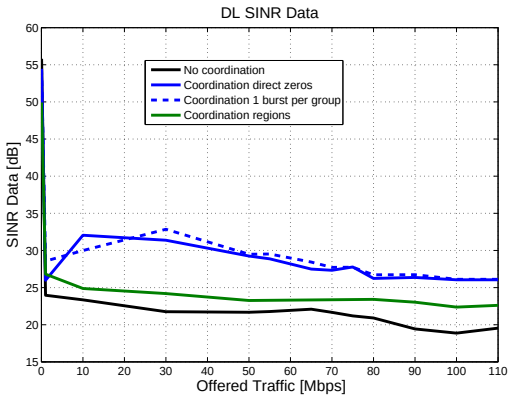

Figure B.11: DL Mean SINR Data

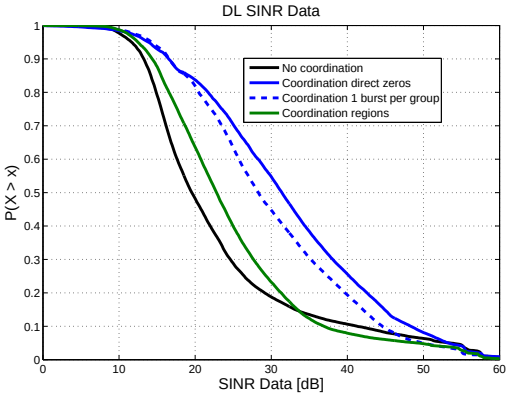

Figure B.12: DL CCDF SINR Data at 10Mbps offered traffic

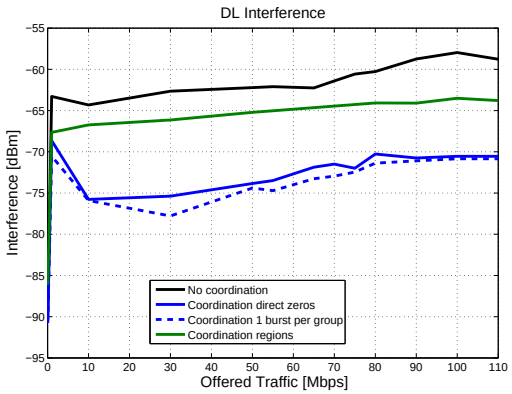

Figure B.13: DL Mean Interference

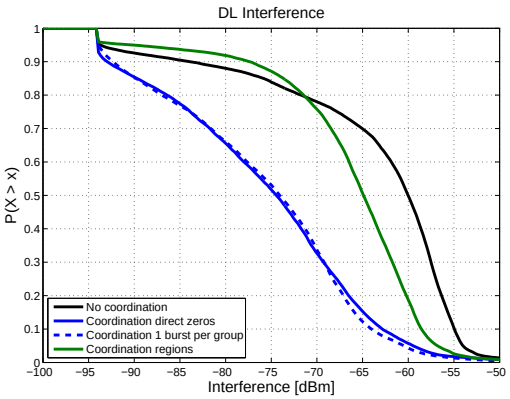

Figure B.14: DL CCDF Inteference at 10Mbps offered traffic

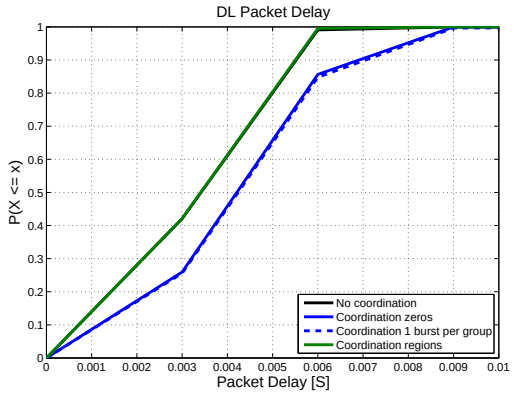

Figure B.15: DL CDF Packet Delay at 10Mbps offered traffic

B.1.2.2 Uplink

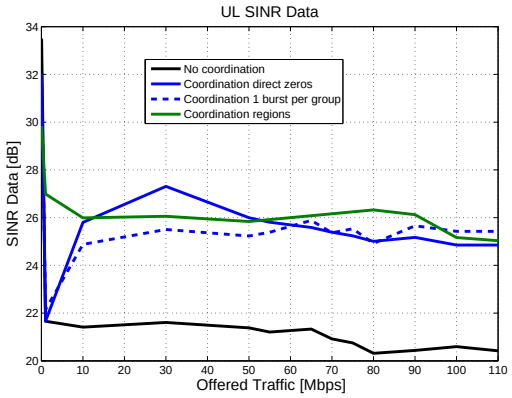

Figure B.16: UL Mean SINR Data

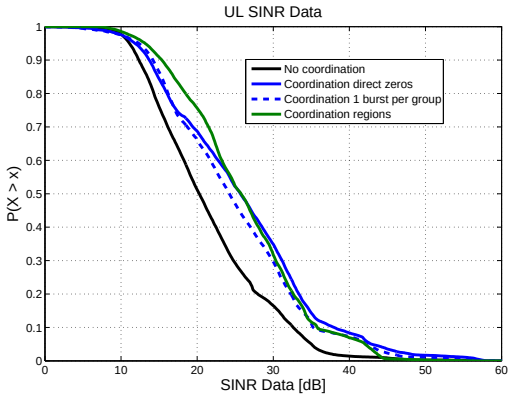

Figure B.17: UL CCDF SINR Data at 10Mbps offered traffic

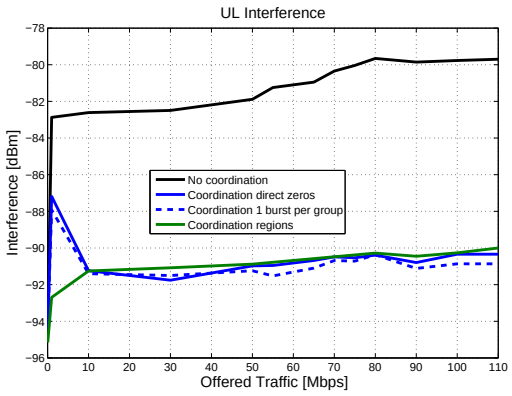

Figure B.18: UL Mean Interference

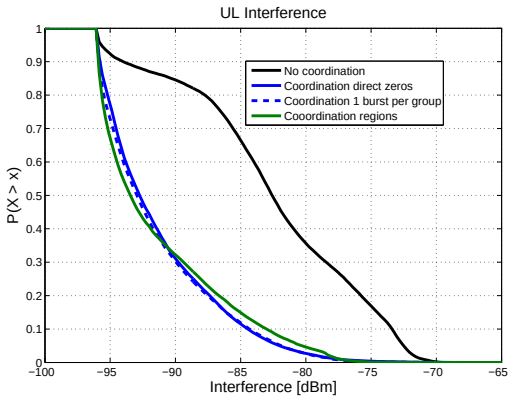

Figure B.19: UL CCDF Interference at 10Mbps offered traffic

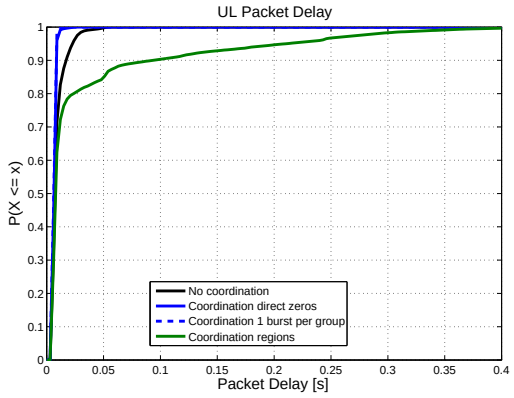

Figure B.20: UL CDF Packet Delay at 10Mbps offered traffic

B.2 VBR scenario

B.2.0.3 Downlink

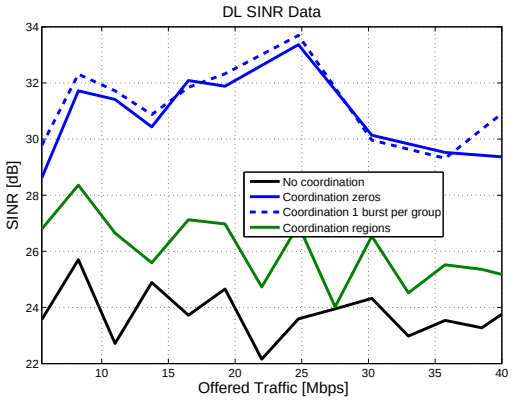

Figure B.21: DL Mean SINR Data

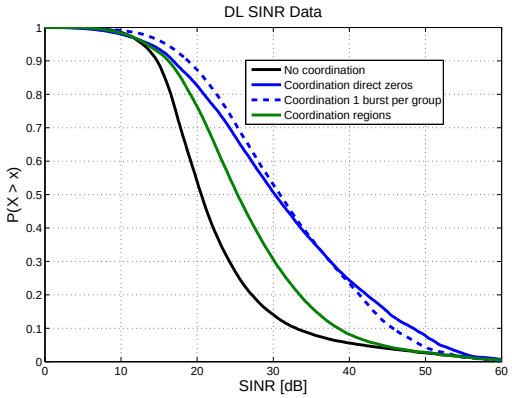

Figure B.22: DL CCDF SINR Data at 10Mbps offered traffic

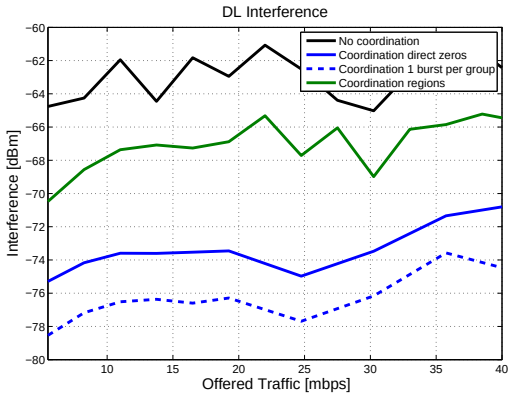

Figure B.23: DL Mean Interference

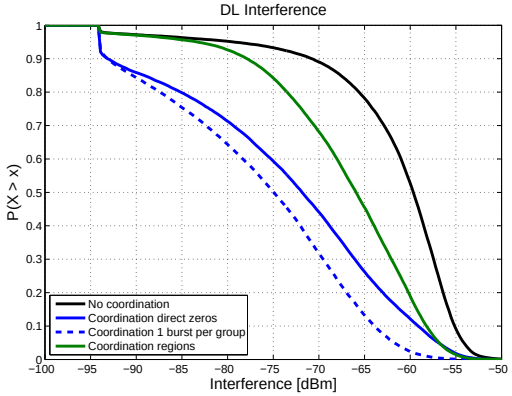

Figure B.24: DL CCDF Interference at 10Mbps offered traffic

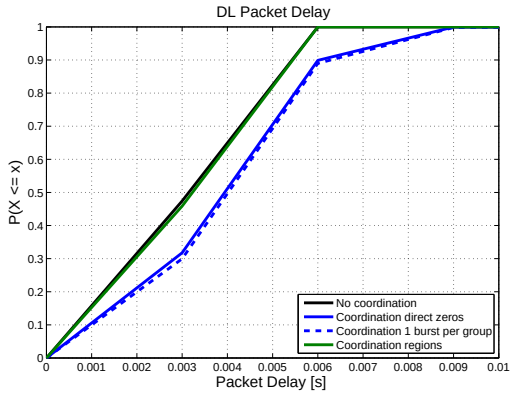

Figure B.25: DL CDF Packet Delay at 10Mbps offered traffic

B.2.0.4 Uplink

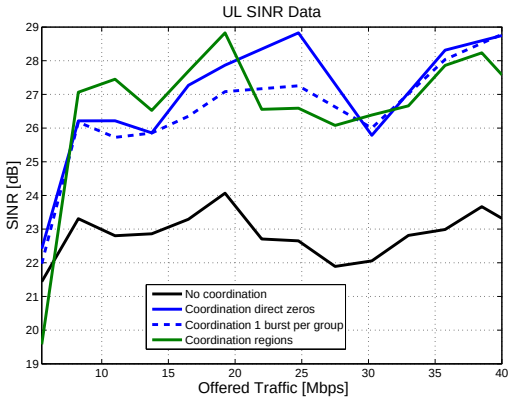

Figure B.26: UL Mean SINR Data

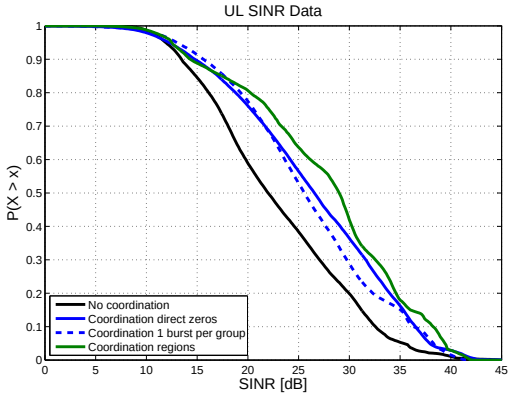

Figure B.27: UL CCDF SINR Data at 10Mbps offered traffic

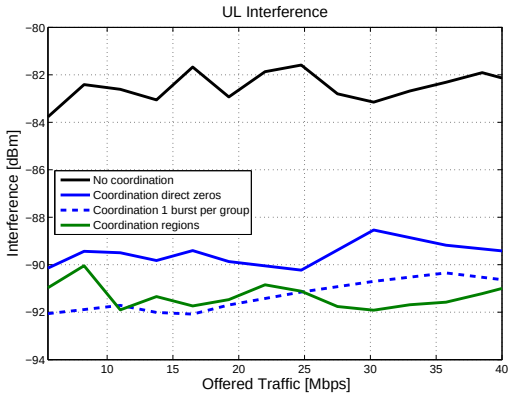

Figure B.28: UL Mean Interference

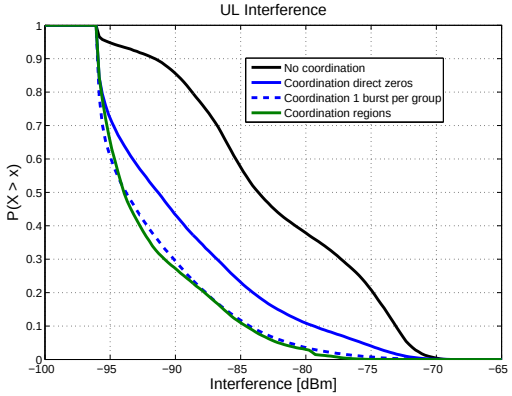

Figure B.29: UL CCDF Interference at 10Mbps offered traffic

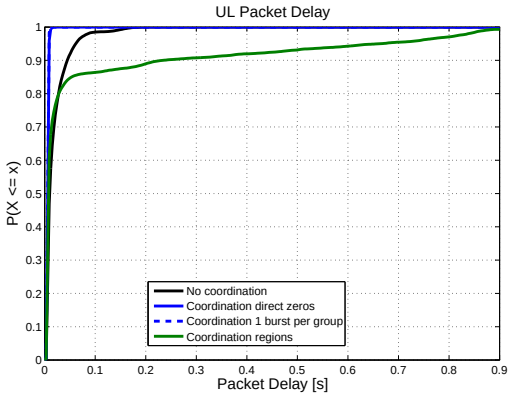

Figure B.30: UL CDF Packet Delay at 10Mbps offered traffic

LIST OF FIGURES

LIST OF TABLES

LIST OF ABBREVIATIONS

2G	2nd Generation
3G	3rd Generation
AWGN	Additive white Gaussian Noise
BER	Bit Error Ratio
BLER	Block Error Ratio
BPL	Broadband over Power Lines
BS	Base Station
BW	Bandwidth
BWA	Broadband Wireless Access
CBR	Constant Bit Rate
CDMA	Code Divison Multiple Access
CRC	Cyclic Redundancy Check
DL	Downlink
DoA	Direction of Arrival
DSL	Digital Subscriber Line
FBW	Fixed Broadband Wireless
FDMA	Frequency Division Multiple Access
FTTH	Fiber to the Home
FU	Functional Unit
FUN	Functional Unit Network
GOP	Group of Pictures
GPS	Global Positioning System
IAT	Inter Arrival Time
IEEE	Institute of Electrical and Electronics Engineers
IMT	International Mobile Telecommunications
ISO	International Organization for Standardization
ITU-R	ITU. Radiocommunication Sector
LOS	Line-of-Sight
MAC	Medium Access Control
MAN	Metropolitan Area Network
MCS	Modulation and Coding Scheme
MIMO	Multiple Input Multiple Output
MISO	Multiple Input Single Output
ML	Maximum Likelihood
MSE	Mean Squared Error
MU MIMO	Multi-User Multiple Input Multiple Output
MVDR	Minimum Variance Distortionless Response
NLOS	Non-Line-of-Sight
OFDM	Orthogonal Frequency Division Multiplexing
OFDMA	Orthogonal Frequency Division Multiple Access
OSI	Open Systems Interconnection
openWNS	open Wireless Network Simulator
PER	Packet Error Rate
PF	Proportional Fair
PHY	Physical Layer
QoS	Quality of Service
RISE	Radio Interference Simulation Engine
Rx	Receiver
RR	Round Robin
SAP	Service Access Point
SC	Single Carrier
SDL	Specification and Description Language
SDMA	Space Division Multiple Access
SIMO	Single Input Multiple Output
SINR	Signal-to-Interference-and-Noise Ratio
SISO	Single Input Single Output
SNR	Signal-to-Noise Ratio
SPEETCL	SDL PErformance Evaluation Tool Class Library
SS	Subscriber Station
SSU	Spatial Super User
TDD	Time Division Duplex
TDMA	Time Division Multiple Access
Tx	Transmitter
UCA	Uniform Circular Array
UL	Uplink
ULA	Uniform Linear Array
VBR	Variable Bit Rate
WiFi	Wireless Fidelity
WiMAC	WiMAX MAC simulator
WiMAX	Worldwide Interoperability for Microwave Access

WLAN	Wireless Local Area Network	WMAN	Wireless Metropolitan Area Network
WLL	Wireless Local Loop		

BIBLIOGRAPHY

[1] Winner ii channel models. ist-4-027756 winner ii d1.1.2 v1.2, 2008. 6.1.5, 6.1.5

[2] IEEE 802.16e Task Group (Mobile WirelessMAN®). 802.16e Project Authorization Request. http://wirelessman.org/tge/, Sep 2004. (document), 2.2

[3] IEEE 802.16e Task Group (Mobile WirelessMAN®). DRAFT Standard for Local and metropolitan area networks. Part 16: Air Interface for Bradband Wireless Access Systems. http://wirelessman.org/tge/, December 2008. 6.1, 7.3

[4] IEEE 802.16m Task Group (TGm). 802.16m Project Authorization Request. http://wirelessman.org/tgm/, Dec 2006. (document), 2.4

[5] IEEE 802.16m Task Group (TGm). IEEE 802.16m Evaluation Methodology Document. http://wirelessman.org/tgm/, Jan 2009. 6.1.5

[6] IEEE 802.16's Relay Task Group. 802.16j Project Authorization Request. http://wirelessman.org/relay/, March 2006. (document), 2.3

[7] A. Alexiou and M. Haardt. Smart antenna technologies for future wireless systems: trends and challenges. Sep 2004. 3.1.2.4

[8] Kwang-Cheng Chen and J. Roberto B. De Marca. *Mobile WiMAX*. John Wiley & Sons Ltd, Chichester, England, 2008. (document), 2.1

[9] R. Compton. *Antennas: Concepts and Performance*. Prentice Hall, 1988. 3.1

[10] Fabian Debus. Performance Evaluation of a Multi-Mode Capable Layer 2 for Relay Enhanced Cells in 4th Generation Mobile Radio Networks. Master's thesis, RWTH Aachen, Lehrstuhl für Kommunikationsnetze, November 2005. 5.1

[11] Sebastian Dreier. Performance Evaluation of Half-Duplex FDD in a Relay Capable Multi Mode MAC Protocol. Master's thesis, RWTH Aachen, Lehrstuhl für Kommunikationsnetze, October 2007. 5.1, 5.1.1, 5.1.2

[12] Jan Ellenbeck. Performance Evaluation of Combined TD-/FD-/SDMA Medium Access Strategies to Support Relay-Enhanced Broadband Cells . Master's thesis, RWTH Aachen, Lehrstuhl für Kommunikationsnetze, April 2006. 3.2

[13] G.J. Foschini and M.J. Gans. On Limits of Wireless Communications in a Fading Enviroment when using Multiple Antennas. *Wireless Pers. Commun.*, 6:311–335, 1998. 3.1.1

[14] M. Fuchs, G. Del Galdo, and M. Haardt. A novel tree-based scheduling algorithm for the downlink of multi-user MIMO systems with ZF beamforming. In *Acoustics, Speech, and Signal Processing, 2005. Proceedings. (ICASSP '05). IEEE International Conference on*, volume 3, 2005. 3.5, 7.3

[15] L.C. Godara. Application of antenna arrays to mobile communications. II. Beamforming and direction-of-arrival considerations. In *Proceedings of the IEEE*, volume 85, pages 1195–1245, 1997. 3.1.2.3

[16] M. Haardt, C. Mecklenbräuker, M. Vollmer, and P. Slanina. Smart antennas for ultra tdd. *Eur. Trans. Telecommun. (ETT), special issue on Smart Antennas, J.A. Nossek and W. Utschick, guest editors*, 12(5):393–406, 2001. 3.1.1

[17] A. Hottinen, O. Tirkkonen, and R. Wichman. *Multi-Antennas Transceiver Techniques for 3G and Beyond*. John Wiley & Sons, Ltd, 2003. 3.1.1

[18] C. Hoymann. *IEEE 802.16 Metropolitan Area Network with SDMA Enhancement*. PhD thesis, Aachen University, Lehrstuhl für Kommunikationsnetze, Jul 2008. (document), 1.2, 3.1, 3.1, 3.1, 3.1.2, 3.1.3, 3.2, 3.3, 3.3.2.1, 3.3.3.2, 4.1.1, 6.1.3

[19] Bong Ho Kim. Text Modification for Draft 802.16m Evaluatin Mothodology: 11.4 Near Real Time Video Streaming. In *Proceedings of the 14th WWRF Meeting*, San Diego, CA, USA, Jul 2005. 6.1.5, 6.2.2

[20] Joseph C. Liberti and Theodore S. Rappaport. *Smart Antennas for Wireless Communications: IS-95 and Third Generation CDMA Applications*. Prentice Hall, 1999. 3.1, 7.3

[21] A. Pauraj, R. Nabar, and D. Gore. *Introduction to Space-Time Wireless Communications*. Cambridge University Press, July 2003. 3.1.1

[22] Rahim Tafazolli. *Technologies for the Wireless Future*. John Wiley & Sons, Ltd, 2006. 3.1.1